NUREG/CR-1359
ORNL/NUREG-65

ornl

OAK RIDGE NATIONAL LABORATORY

UNION CARBIDE

Fabrication of Sensors for High-Temperature Steam Instrumentation Systems

A. J. Moorhead
M. B. Herskovitz
C. S. Morgan
J. J. Woodhouse
R. W. Reed

Prepared for the
U.S. Nuclear Regulatory Commission
Office of Nuclear Regulatory Research
Under Interagency Agreement DOE 40-551-75

OPERATED BY
UNION CARBIDE CORPORATION
FOR THE UNITED STATES
DEPARTMENT OF ENERGY

Printed in the United States of America. Available from
National Technical Information Service
U.S. Department of Commerce
5285 Port Royal Road, Springfield, Virginia 22161

Available from

GPO Sales Program
Division of Technical Information and Document Control
U.S. Nuclear Regulatory Commission
Washington, D.C. 20555

NUREG/CR-1359
ORNL/NUREG-65
Distribution
Category R5

Contract No. W-7405-eng-26

METALS AND CERAMICS DIVISION

FABRICATION OF SENSORS FOR HIGH-TEMPERATURE STEAM INSTRUMENTATION SYSTEMS

A. J. Moorhead, M. B. Herskovitz, C. S. Morgan,
J. J. Woodhouse, and R. W. Reed

Manuscript Completed — February 29, 1980

Date Published — May 1980

Prepared for the
U.S. Nuclear Regulatory Commission
Office of Nuclear Regulatory Research
Washington, DC 20555
Under Interagency Agreement DOE 40-551-75
NRC FIN No. B0413

Prepared by the
OAK RIDGE NATIONAL LABORATORY
Oak Ridge, Tennessee 37830
operated by
UNION CARBIDE CORPORATION
for the
DEPARTMENT OF ENERGY

CONTENTS

FABRICATION OF SENSORS FOR HIGH-TEMPERATURE STEAM INSTRUMENTATION SYSTEMS

A. J. Moorhead, M. B. Herskovitz, C. S. Morgan, J. J. Woodhouse, and R. W. Reed

ABSTRACT

A series of instruments is under development at ORNL for measurement of two-phase (steam and water) flow parameters in out-of-reactor safety tests that simulate a loss-of-coolant accident in a pressurized water reactor. To enable these instrument sensors to be built, we have developed a unique ceramic-to-metal seal system, which will withstand relatively short-time exposure to 800°C (1470°F) steam and remain leaktight after repetitive thermal transients of 300°C/s (540°F/s). A ceramic insulator was developed after we found that no commercial insulating material met the steam compatibility, impermeability, or thermal shock requirements. This material is basically aluminum oxide containing a very fine dispersion of platinum nodules, which greatly enhance the thermal shock resistance of the hot-pressed cylinders. This insulator has little or no weight change on exposure to steam at 650 to 750°C (1200–1380°F) for over 100 h and has a helium leak rate of less than 0.005 mm^3/s after 25 quenches from 520°C (970°F) air into water at 80°C (175°F).

The ceramic-to-metal seal system consists of this insulator directly brazed to one or more metallic transition pieces with an ORNL-developed brazing filler metal having composition 49 Ti–49 Cu–2 Be (wt %). The transition, which is platinum or a combination of platinum and type 446 ferritic stainless steel in some cases, is necessary to accommodate the large difference in coefficients of thermal expansion between that of the insulator and that of the stainless steel sensor housings or electrical cables. These seal assemblies have excellent resistance to high-temperature steam oxidation and thermal transients.

Thirteen highly complex instrumented guide tube assemblies, each containing a number of these ceramic-to-metal seals, have been fabricated, and seven were shipped to Germany for testing in an out-of-reactor safety test facility. Each assembly consisted of two pairs of sensor subassemblies at each of two locations along a 13.7-mm-diam by 4.3-m-long (0.54-in. by 14-ft) stainless steel tube. Eight 3.18-mm-diam (0.125-in.) triaxial cables, each having a ceramic-to-metal seal brazed on one end, passed through the bore of the tube and were connected by a laser weld to the sensor electrodes.

In addition to the ceramic-to-metal seal development necessary for guide tube fabrication, procedures were also developed for (1) laser welding of sensor subassemblies into the tube wall, (2) induction brazing of four stainless-steel-sheathed thermocouples through the tube wall, and (3) furnace brazing of the eight triaxial cables, four thermocouples, and a vent tube where they passed through the upper end of the guide tube.

INTRODUCTION

The effectiveness of the emergency core cooling systems of water-cooled nuclear reactors has been the subject of extensive experimental studies and theoretical analysis for many years. Thus, the thermohydraulic phenomena that occur after a postulated break in a primary coolant line of a pressurized water reactor during the blowdown, refill, and reflood phases are currently being studied in various projects around the world. Although some of the necessary research requires actual in-reactor testing, many of the studies of thermohydraulic performance at prototypic steady-state and transient operating conditions can be conducted on simulated segments of core assemblies by using high-performance, electrically heated fuel rod simulators in place of the radioactive fuel rods. A number of such experiments have been conducted over the years. Even though in some cases the test bundles have been fairly large, all these tests can still be regarded as studies on unidimensional thermohydraulic effects. Therefore, a joint program to study three-dimensional phenomena in the upper plenum and core of a pressurized water reactor during the reflood stage of a loss-of-coolant accident has been initiated by the United States Nuclear Regulatory Commission in cooperation with its counterparts in West Germany and Japan. The role of ORNL under the Advanced Instrumentation of Reflood Studies (AIRS) Program in this effort is to develop and supply instrumentation systems for measurement of three-dimensional two-phase (steam and water) flow parameters in two German and two Japanese nonnuclear reflood test facilities.

Several different types of sensors and configurations are under development, but the subject of this report is one of a type known as an impedance probe. In this device the electrical impedance between two electrodes extending into the subchannel spacing between three fuel rod simulators (Fig. 1) is measured to provide information on the local ratio of steam and water. By cross correlation of the electrical output of two axially separated sensors, the velocity and direction of flow of the fluid can be determined. Although ORNL has conducted various activities involved with the development of the impedance probe, including the determination of specific electrode geometry and spacing, the design and construction of

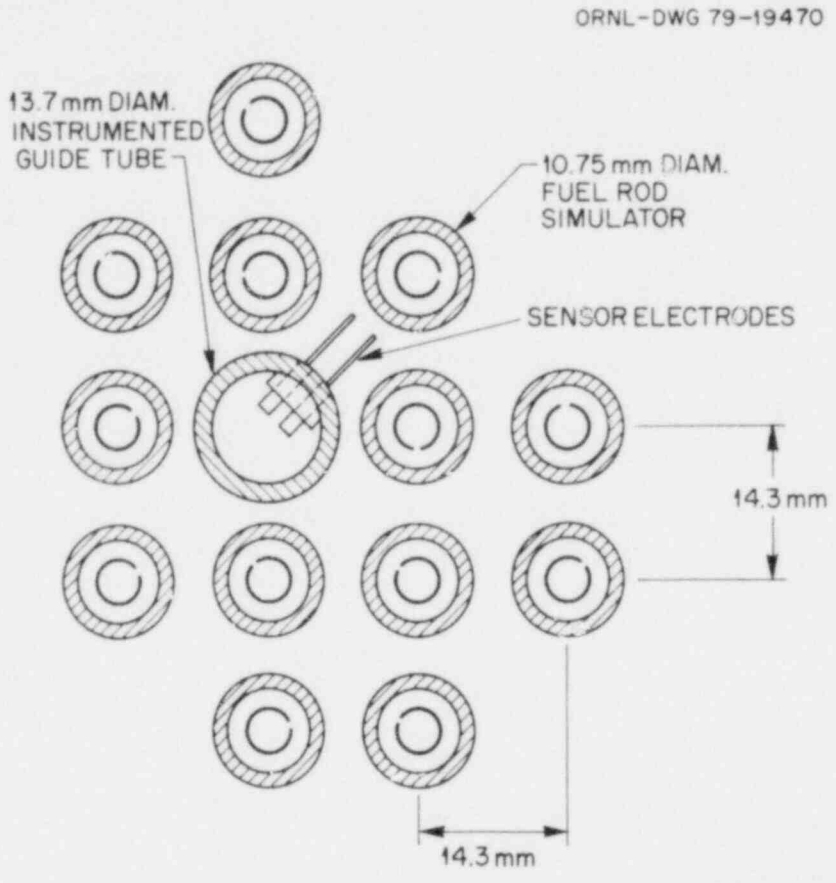

Fig. 1. Plan View of a Portion of the PKL II Test Bundle Showing the Orientation of the Impedance Sensors with Respect to Three Heated Fuel Rod Simulators.

instruments to excite and monitor the sensors, and the ultimate testing of assemblies in a steam-water system,[1] these topics will not be included in this report. What will be included are our efforts in taking the conceptual requirements for an impedance sensor and translating these into an instrumented test rod, which on the one hand was capable of being fabricated and on the other was a functionally acceptable portion of an instrumentation system. The particular devices made were specifically for a 340-rod German reflood test facility known as Primärkreislauf (PKL), and hence some features such as overall dimensions of the instrumented rods were tailored to that system. However, most of the materials development and testing activities as well as the general joining concepts can be applied to many other reactor safety test programs. For instance, we have

recently begun development of fabrication techniques for two types of sensors for the Blowdown Heat Transfer Program here at the Laboratory.

GENERAL REQUIREMENTS FOR PKL PRONG PROBES

As one might expect, the conditions to which a sensor will be exposed in a reflood test system are severe. After a postulated loss-of-coolant accident in a reactor core, the temperature of the fuel rods will rise significantly after the blowdown until the emergency core cooling (ECC) water is introduced during the refill and reflood phases. As the result of reflood, the temperature of the fuel rod simulators and the instrumented rods will then drop very rapidly, causing a very severe thermal shock to the components. Accordingly, the typical operating sequence for the German PKL Core II test for which sensors were produced will be as follows:

1. 2–3 h heatup from ambient to 150°C (300°F) with slightly superheated steam,
2. variable hot standby period with 4 h maximum at about 200°C (390°F),
3. power applied to fuel rod simulators to heat up to 560 to 700°C (1040–1290°F) in about 10 min,
4. actual reflood test with power and ECC injection, duration about 10 min with maximum temperature at the core hot spot of 950°C (1740°F) – see curve on Fig. 2,
5. vessel cooldown from about 150°C to ambient requiring about 8 h – the water is drained from the vessel within the first hour of this period,
6. four weeks shutdown between tests with 100% relative humidity air in vessels and piping.

The magnitude of the maximum thermal transient to be expected in the PKL II tests was estimated (on the basis of some data from the PKL I bundle) to be a drop of about 300°C/s (540°F/s) for 0.5 s. Therefore, we set the criteria for the total steam-water exposure of our sensors as:

Time at 800–900°C:	5 h total (50 cycles)
Thermal Shock:	50 cycles of 2 s each [300°C/s (540°F) for 0.5 0.5 s]
Time at 200°C:	200 h total
Time at ≥150°C:	600 h total
Time loop water filled:	50 h total at about 150°C (300°F)

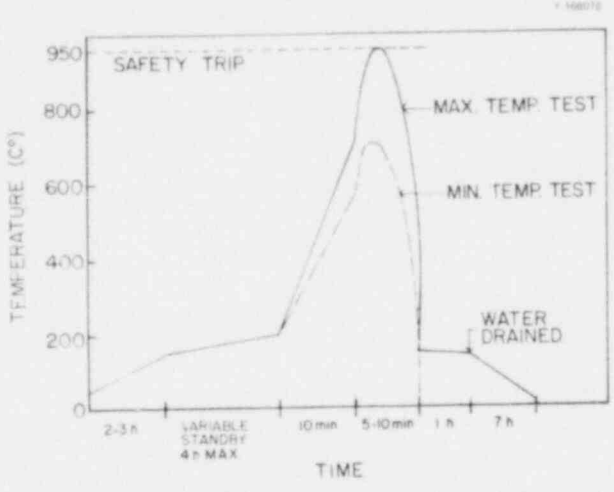

Fig. 2. Typical Test Cycle in the PKL Reflood Facility. The temperatures shown are the maximum core temperature, whereas the impedance rod temperatures will be approximately 200°C (360°F) less.

SENSOR GEOMETRY

Although up to this point we have mentioned only a single type of impedance sensor for the PKL tests, we were called upon to fabricate actually two separate but related geometries developed by our instrumentation and two-phase flow specialists. The first was known as a "prong probe." It consisted of two sets of parallel and electrically isolated electrodes, with each pair spaced 3.05 mm (0.120 in.) center-to-center and with the two sets at a distance of 9.52 mm (0.375 in.) from each other. The second design was called a "flag probe." It was made up of four pairs of electrodes, with two pairs close to each other and separated from the other two pairs by a distance of 19.05 mm (0.750 in.). As its name implies, the flag probes had small strips of metal stretched between electrodes of each pair to increase the magnitude of the output signal by presenting a larger sensor area to the fluid. The general geometry of

both types of probe is shown in Fig. 3. Note that one electrode in each pair in a flag probe serves only to support an end of the sensor, so that both types require a total of four electrical leads to monitor the output signal. Thus in most respects the probes are very similar and in general will be discussed below as one.

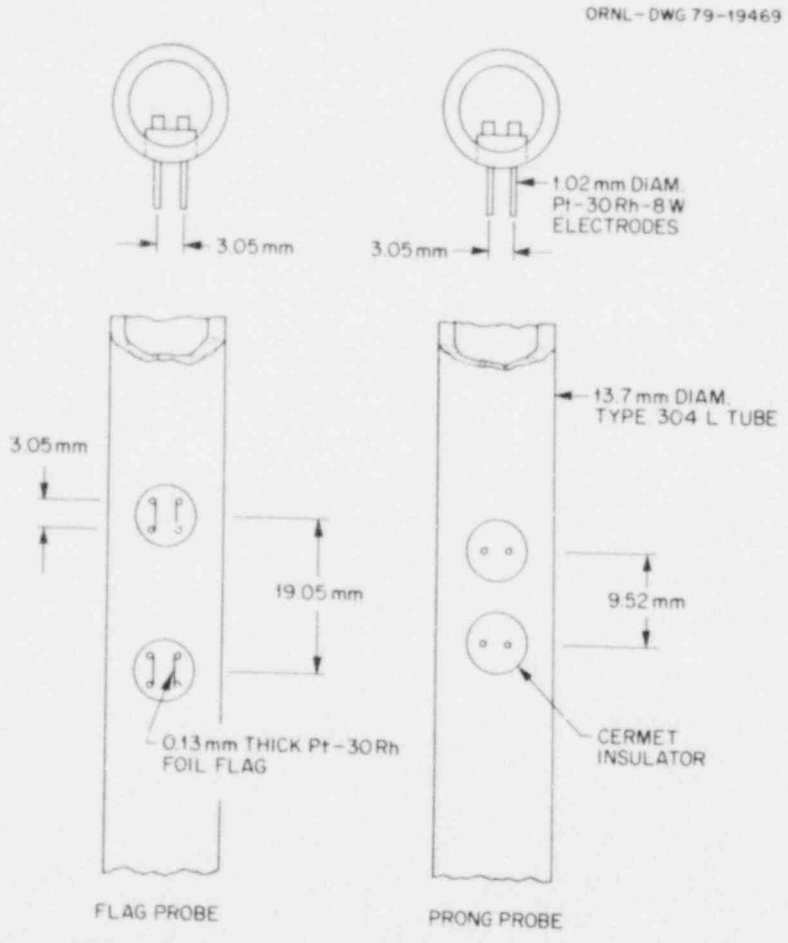

Fig. 3. Configurations of Two Types of Impedance Probe Sensors Fabricated for the PKL Reflood Facility.

The other predetermined features of the instrumented assembly were the desire to have a thermocouple above and below each sensor location, and the external package requirements for the device. The required package was a type 304L stainless steel tube with dimensions of 13.69 mm OD. by 1.17 mm wall by 4.32 m length (0.539 by 0.046 by 170 in.). Also each instrumented rod had to house prong- or flag-probe subassemblies

at two locations (to simultaneously monitor two levels in a given flow channel), so that the total electrical cable requirements for a given rod were four sheath-type thermocouples and eight triaxial leads. The reason for use of triaxial leads running to each electrode is an instrumentation requirement and not a matter for discussion in this paper. Suffice it to say that the leads were in the form of 3.18-mm-diam (0.125-in.) stainless-steel-sheathed cables with a 1.58-mm-diam (0.062-in.) inner sheath and a 0.69-mm-diam (0.027-in.) central conductor. Each of the three conductors was insulated from the others by a layer of aluminum oxide.

CERAMIC-TO-METAL SEAL SYSTEM INSULATOR DEVELOPMENT

The requirement for an array of electrodes electrically isolated from each other and from the tubular housing or rod necessitated the development of a ceramic-to-metal seal system that would withstand the PKL conditions of steam at a temperature of 850°C (1560°F) and a pressure of 0.62 MPa gage (90 psig). Of course one of the most challenging aspects of this problem was to develop a seal system that would maintain its integrity even after many thermal transients. Although ceramic-to-metal seals are used in a number of commercial areas, we were unaware of any that would meet our needs of high-temperature steam oxidation resistance, leaktightness, and thermal shock resistance. Therefore, we undertook the development of our own specialized system.

The selection of an insulating material was begun by screening a number of commercially available ceramics in a thermal shock test. This test consisted of heating specimens in air at a temperature of 520°C (970°F) and then dropping them into water at 80°C (175°F). Although higher furnace temperatures were initially used, we concluded that these conditions provided a sufficiently rigorous test. The approximate rate of cooling, determined by attaching a thermocouple to the specimen and recording the temperature during quenching with a transient recorder, was about 600°C/s (1080°F/s). Although this was a more severe shock than the 300°C/s (540°F) transient that we assumed would be seen in the German system, we elected to use this test anyway to provide a margin of safety, as the PKL data were somewhat limited. The effect of thermal shock was

evaluated on the basis of cracks as observed through a stereo microscope at a magnification of 30×. Dye penetrant tests were not used since many of the ceramics tested were porous. The results of this first round of tests are given in Table 1.

Table 1. Commercial Materials Tested for Thermal Shock

Material	Coefficient of Linear Thermal Expansion (K^{-1})	Density (% of theoretical)	Results of Thermal Shock Tests[a]
Aluminum oxide[b]	6.5×10^{-6}	>99	Microscopic cracks visible after 1 quench
Beryllium oxide	8	>99	Microscopic cracks visible after 1 quench
Beryllium oxide	8	>80	Cracks visible after 2 or 3 quenches
Cordierite (Alsimag 701) $2MgO \cdot 2Al_2O_3 \cdot 5SiO_2$	3.3	99	Cracks visible after 2 or 3 quenches
Cordierite (Alsimag 447)	1.5	>85	No cracks after 30 quenches
Rosolite ($Al_2O_3 \cdot 4SiO_2 \cdot 9Li_2O$)	<1	80	No cracks after 30 quenches
Rosolite	<1	99	Microscopic cracks visible after 2 quenches
Si_3N_4	2.8	>90	Small cracks near edge after 10 quenches
Quartz	1.9	100	No cracks after 10 quenches
Macor (Corning glass ceramic)	9.4	100	Broke into pieces after 2 quenches

[a]Quenching from 520°C (970°F) into water at 80°C (175°F).

[b]Several types of Al_2O_3 were tested (including sapphire); all cracked.

Several observations were made after these tests concerning the thermal shock resistance of commercial ceramic materials. First of all, note that in general only those materials that had both a low coefficient

of thermal expansion and relatively low density (percent of theoretical) were able to survive even two or three of these quenches without visibly cracking. The one exception to this trend was the quartz, but we have data that show that this material is subject to dissolution or leaching in hot water. We confirmed this tendency in our quenching tests by noting that the quartz sample was "frosted" after only the short hot water exposure experienced in three or four quenches.

Because of the disappointing results in thermal shock testing of commercial materials, we embarked on a task to develop a more suitable insulator. Prior study of the preparation of ceramic bodies with three-dimensional networks of thin metal foils permeating them suggested testing cermets with finely dispersed metal particles.[2] The thin-film cermets had good thermal shock characteristics by virtue of the oxide enclaves being held in a continuous metal matrix but had far too high electrical conductivity for an AIRS insulator. However, we thought that if the metal content was dispersed as fine particles rather than as thin films it would continue to increase toughness of the ceramic while not significantly affecting the electrical conductivity.

Cermets intended to serve as insulators were prepared by hot-pressing ceramic powder containing finely dispersed metal powder. The ceramic-metal powder was prepared by coating the ceramic particles with a metal precursor compound and decomposing under conditions that resulted in fine metal particles dispersed on the ceramic particle surface.

The first cermet made was Al_2O_3–2.6 vol % Fe prepared by decomposing ferric nitrate deposited on a relatively coarse Al_2O_3 powder. The decomposition was at 800 to 900°C (1470 to 1650°F) for 10 min in a hydrogen atmosphere. The Al_2O_3-Fe cermet powder was hot-pressed at 41.4 MPa (6000 psi) and 1400°C (2550°F) for 30 min to a density equivalent to about 85% of theoretical. This sample showed no sign of cracking or other deterioration in ten quenches; however, during several days treatment in high-temperature steam [400 to 650°C (750 to 1200°F)] its weight slowly increased, indicating that the iron particles were oxidizing.

We then decided to prepare cermet insulators with a noble metal, platinum, so that the danger of metal oxidation would be removed. Alumina powder was slurried in an aqueous solution of $PtCl_4$. The water was removed

slowly by heating with continuous agitation. Agitation until the powder is fluffy is necessary to maintain a uniform distribution of the $PtCl_4$ as the water is removed. The dried powder was heated to 900°C (1650°F) in a hydrogen atmosphere for 10 min to convert $PtCl_4$ to metal. At this conversion temperature platinum has no tendency to form a film on the particle surface.

Initially the Al_2O_3-Pt powder was prepared from "large" Al_2O_3 particles, 30 to 70 μm. This resulted in a hot-pressed specimen of about 85% of theoretical density. We first thought that the less dense material would have superior thermal shock resistance, and the 85%-dense specimens never cracked during thermal shock tests. However, using 1- to 3-μm Al_2O_3 powders and hot-pressing at 82.7 MPa (12,000 psi) and 1600°C (2910°F) for 15 min we obtained almost theoretically dense Al_2O_3-Pt specimens. Significantly, these samples also exhibited high resistance to thermal shock. Apparently the thermal shock stresses exceed the strength of the material but are relieved by numerous small cracks. Platinum particles limit crack growth and Pt-to-Al_2O_3 bonding enables the structure to retain a high integrity for many quenches.

A large number of cermet blanks were subsequently fabricated by hot-pressing mixtures of aluminum oxide powders containing very small amounts of metallic "binders." The volume of the metal and the firing temperature were controlled such that the oxide particles were not held in a continuous metal matrix but instead were separated by a very fine dispersion of metal nodules, as shown in Fig. 4. As can be seen from the test data for some of these materials in Table 2 (which also includes results for some experimental ceramics under development at the Oak Ridge Y-12 Plant),[3] these experimental materials have a high degree of resistance to thermal shock. However, as mentioned previously, the Al_2O_3–2.6 vol % Fe slowly oxidized during the high-temperature steam compatibility tests and was, therefore, removed from consideration.

Because the platinized alumina cermet material behaved favorably in the preliminary tests we set about to optimize this material through minor changes in platinum content and hot-pressing conditions. More rigorous tests were also conducted by exposing samples to high-temperature steam

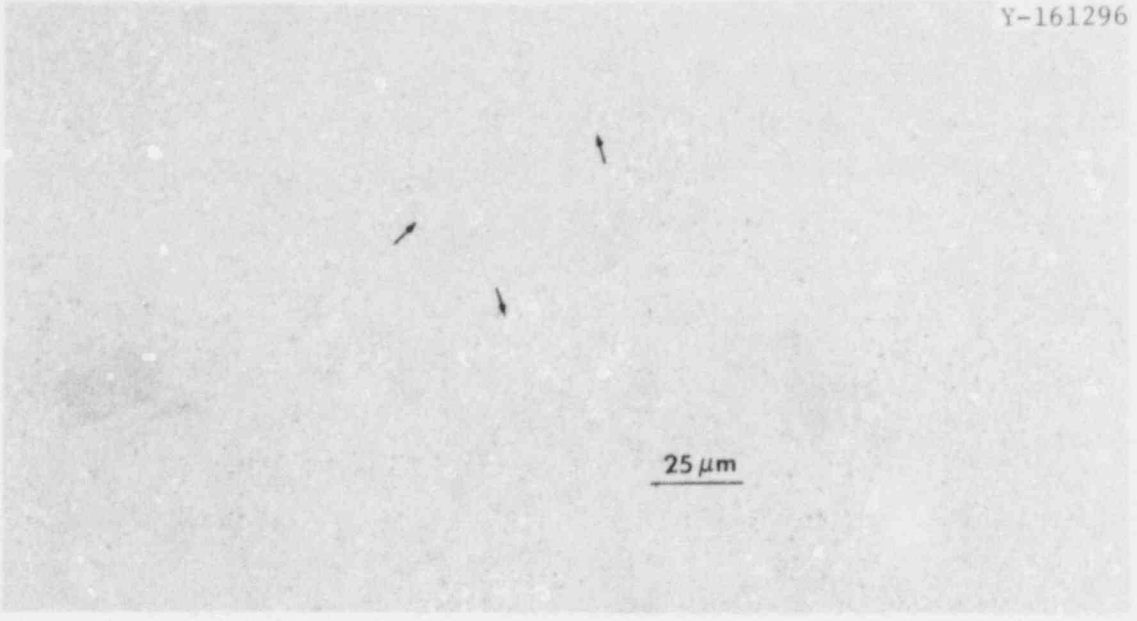

Fig. 4. Platinized Alumina Cermet Showing the Fine Dispersion of Platinum Nodules (Arrows) Separating the Oxide Particles.

Table 2. Experimental Materials Tested for Thermal Shock

Material	Coefficient of Linear Thermal Expansion (K^{-1})	Density (% of theoretical)	Results of Thermal Shock Tests[a]
Al_2O_3–2.6 vol % Fe	7×10^{-6}	85	No cracks after 10 quenches
Al_2O_3–0.5 vol % Pt	6.5	85	No cracks after 10 quenches
Al_2O_3–0.5 vol % Pt	6.5	99	No cracks after 10 quenches
Al_2O_3–0.25 vol % Pt	6.5	99	No cracks after 10 quenches
Al_2O_3–1 vol % Pt	6.5	99	No cracks after 10 quenches
ZrO_2–0.5 vol % Pt	11.0	85	Cracks visible after 3 quenches
Ta_2WO_8	−2.1	>90	No cracks after 10 quenches
Hf-Ta_2WO_8	0.0	>90	No cracks after 10 quenches

[a]Quenching from 520°C (970°F) air into water at 80°C (175°F).

[b]Does not leak helium until after approximately 50 thermal shock tests.

and up to 55 thermal shocks. Our criteria for the steam exposure was a minimal weight loss, and the resistance to thermal transients was determined by a helium permeability check. The latter test consisted of clamping a ceramic blank in a rubber hose, pressurizing one side with helium at 0.17 MPa gage (25 psig) and immersing the exposed surface in ethanol. After a number of iterations of hot-pressing samples and testing, a material was developed that had little or no weight change after exposure to steam at 650 to 750°C (1200 to 1380°F) for over 100 h and would not display a helium leak after 20 or more quenches. A typical metallographic sample of this material (Fig. 5), which contains a 0.5 vol % Pt dispersed among fine particles of aluminum oxide, after 20 quenches reveals a few microcracks, but they are so small and few that they apparently do not interconnect to form a leak path. After this cermet has

Fig. 5. Platinized Alumina Cermet Insulator After 20 Quenches from 520°C (970°F) Air into Water at 80°C (175°F). Although the structure contains some microcracks, they typically do no interconnect (after this many thermal shocks) to form a major leak path.

been quenched up to 50 times, it generally shows some helium bubble formation in the alcohol immersion test, but the overall integrity of the material is still excellent. Several of the hot-pressed blanks of platinized alumina are shown in Fig. 6.

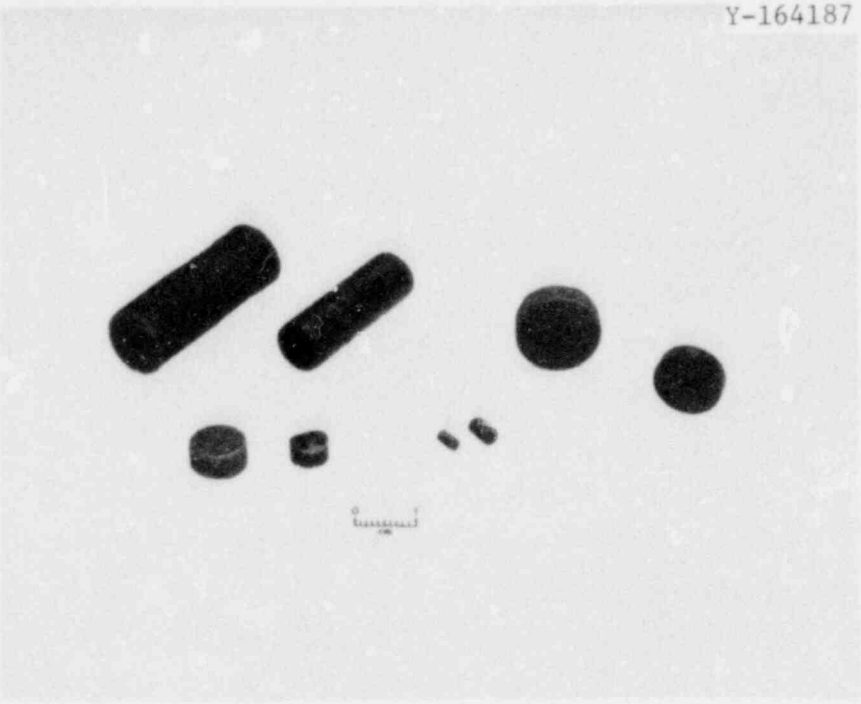

Fig. 6. Hot-Pressed Blanks of Platinized Alumina Cermet Both Before and After Grinding into Insulator Parts.

BRAZING DEVELOPMENT

Parallel to the search for an acceptable insulator material for our ceramic-to-metal seal system was the testing and selection of a brazing technique and filler metal for joining the insulator to the electrode posts and the stainless steel housing. The most difficult aspect of the joint, of course, is in brazing to make the ceramic-to-metal seal. Two main techniques are available for consideration. In one the ceramic is first coated with a metallic material and the braze is subsequently made to that coating. Coatings can be applied by vapor or ion plating or by the decomposition of a hydride slurry (e.g., titanium hydride) during the

brazing cycle itself. One of the most commonly used coatings in commercial practice[4,5] is known as moly-manganese and is applied as follows. A proprietary slurry made up of powdered molybdenum and/or molybdenum oxide, manganese, and various oxides is applied to the ceramic and fired in a wet H_2-N_2 atmosphere at a high temperature, typically 1400°C (2550°F). Some of the oxides are reduced to the metal and others combine among themselves and with the ceramic to form a viscous melt. On solidification this glassy phase bonds the porous sintered metal (molybdenum) to the ceramic. The coating is then plated with a very thin layer of nickel or copper to form a readily wettable layer for subsequent brazing. Commonly used filler metals with this technique are the silver-base alloys such at BAg-8 (Ag–28% Cu), BAu-4 (Au–18% Ni), or pure copper.

In the second technique the braze is made directly to the metal and ceramic with a filler metal containing an active metal such as titanium or zirconium. In some cases the alloy is in the form of a composite of nickel with a titanium core, which on heating above 955°C (1750°F) forms a nickel-titanium eutectic filler metal. Alloys can also be prepared in conventional ways by arc melting the constituents to form a button or ingot, which is then processed into a usable form for preplacement at a joint by swaging into wire, rolling into foil, or crushing into powder. A number of active metal brazing alloys have been developed at ORNL specifically for wetting of ceramics and graphite,[6–8] so we began our brazing alloy selection process by testing some of these materials for wetting and flow on the cermets and ceramics being considered at the time.

As there was some concern that these active metal alloys would not survive the steam oxidation conditions of PKL, we also initiated a task on precoating of the ceramic with either a sputtered layer of platinum or a conventional moly-manganese coating. The precoating techniques have a major advantage over the direct brazes in that the extent of alloy wetting is determined by the area coated. In a direct braze there is sometimes extensive alloy flow, which could provide an undesired electrical path between the probes in our sensors. The moly-manganese coating, on the other hand, has the potential for unacceptable corrosion behavior (due to the poor oxidation resistance of the molybdenum) unless it is completely covered by a corrosion-resistant filler metal.

Before a brazing filler metal is selected the materials to be joined are generally known. However, because of the extreme tightness of our schedule the insulator material had not been selected at the time we initiated our brazing study. As far as the other side of the joint was concerned, all that was known was that the ultimate housing was a type 304L stainless steel tube. A major problem in any brazement between dissimilar materials is the difference between the coefficients of thermal expansion of the two materials. If the braze gap increases significantly on heating because of a large mismatch in coefficient the brazing filler metal may not be drawn into the joint by capillary flow. On the other hand, if the materials and configuration are such that the gap becomes too small, the alloy may not be able to penetrate the joint. In normal practice in brazing of dissimilar materials, the material having the greater coefficient of expansion is made the outer member of the joint, and joint tolerances are held such that the gap between the surfaces does not become too great for capillary flow. The general problem of brazing of dissimilar materials is generally more difficult when one part of the joint is a ceramic. Although this is not always the case, metals usually have a greater coefficient of thermal expansion than ceramics, as can be seen in Fig. 7. The problem in metal-to-ceramic joints is compounded by the little or no ductility of ceramics and their relative weakness under tensile loading. These two characteristics are generally accommodated for in commercial ceramic-to-metal seals by using a metal having relatively low

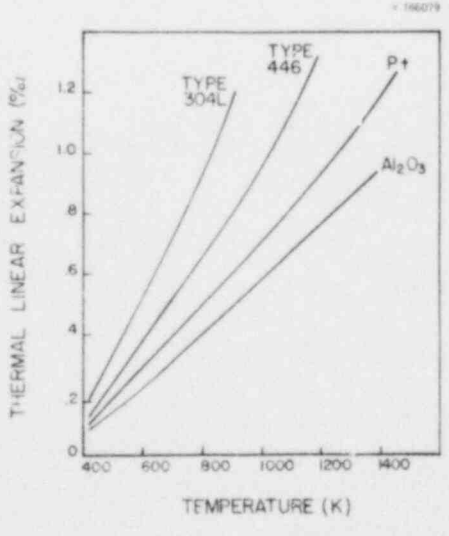

Fig. 7. Thermal Expansion of Several Metals Compared with Alumina.

coefficient of expansion (such as Kovar*) or one of the refractory metals and by using thin metal sections (Fig. 8) that can deform easily when stressed. One of these options was not open to us as the refractory metals (e.g., W, Ta, Nb, and Mo) have poor resistance to high-temperature oxidation and would therefore, not be suitable for use in our sensors.

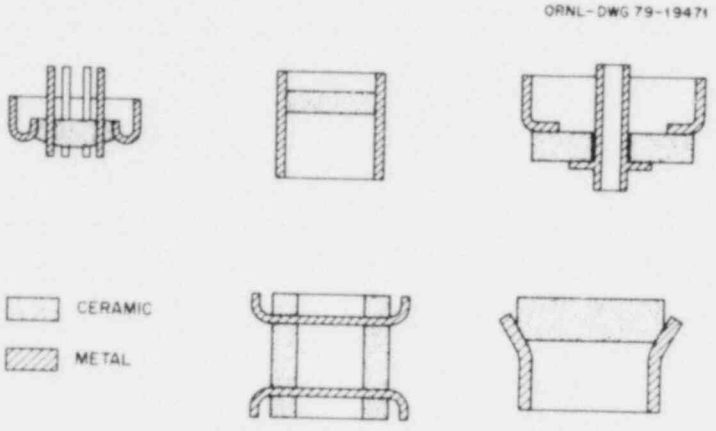

Fig. 8. Typical Geometry of Conventional Ceramic-to-Metal Seals.

Our initial braze screening tests were on chunks or disks of the various ceramics under consideration brazed to t'e top of pieces of potential metallic members as typified by the samples in Fig. 9.

---

*"Kovar" is a registered trademark of Westinghouse Electric Company for the alloy Fe—29% Ni—17% Co.

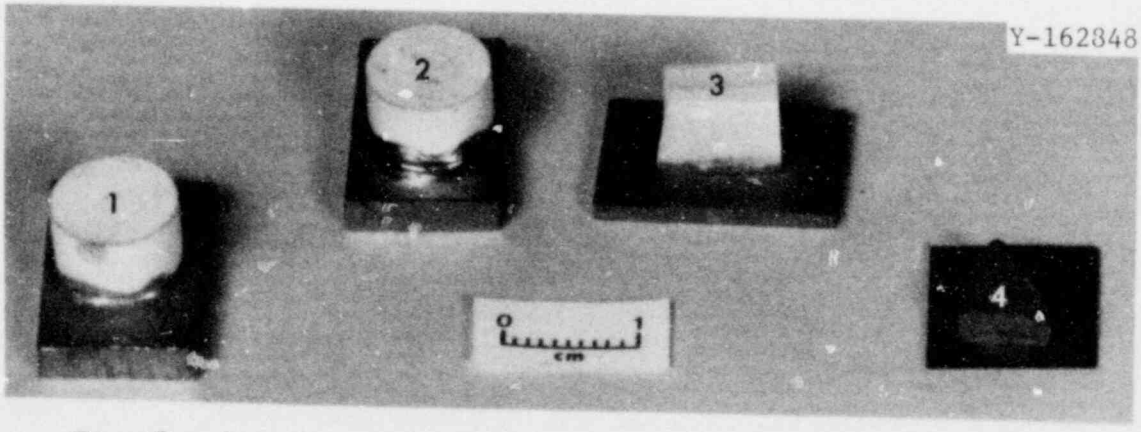

Fig. 9. Ceramic-to-Metal Braze Samples Used in Filler Metal Screening Tests. (1) Aluminum oxide to Kovar with 68Ti-28Ag-4Be filler metal, (2) alumina-Kovar, 49Ti-49Cu-2Be, (3) rosolite-molybdenum, 72Ti-28Ni, (4) cordierite-tantalum, 49Ti-49Cu-2Be.

Although this arrangement does not appear to produce as favorable a stress condition on the joint and ceramic (as would for instance having a cylindrical ceramic button brazed within a hole in the metal), we were mainly testing wetting and flow behavior and therefore elected not to spend the time and money machining specimens. The results of some of these initial brazing tests are given in Table 3. Note that in some cases

Table 3. Results of Brazing Filler Metal Wetting Tests on Various Ceramic/Metal Combinations[a]

AIRS Braze	Base Materials	Filler Metal Composition (wt%)	Brazing Temperature (°C)	Brazing Temperature (°F)	Results Based on Visual Examination
1	Al_2O_3-Kovar[b]	49Ti-49Cu-2Be	980	1800	Excellent wetting and flow, no cracking
2	Al_2O_3-Kovar	68Ti-28Ag-4Be	1040	1900	Good wetting and flow
3	Al_2O_3-Kovar	48Ti-48Zr-4Be	1050	1920	Fair wetting, joint failed on cooling
4	Al_2O_3-Kovar	72Ti-28Ni[c]	1140	2080	Fair wetting, filler metal oxidized
9a	Rosolite[d]-Kovar	72Ti-28Ni[c]	1140	2080	Good wetting, overly porous ceramic soaked up filler metal, joint failed on cooling
9b	Cordierite[e]-Kovar	72Ti-28Ni[c]	1140	2080	Good wetting, overly porous ceramic soaked up filler metal, joint failed on cooling
9c	Si_3N_4[f]-Kovar	72Ti-28Ni[c]	1140	2080	Good wetting, joint failed on cooling
10	Si_3N_4-Ta	72Ti-28Ni[c]	1140	2080	Good wetting, joint failed on cooling
11	Rosolite-Ta	72Ti-28Ni[c]	1140	2080	Good wetting, overly porous ceramic soaked up filler metal, joint failed on cooling
12	Cordierite-Ta	72Ti-28Ni[c]	1140	2080	Good wetting, overly porous ceramic soaked up filler metal, joint failed on cooling
20	Cordierite-Ta	49Ti-49Cu-2Be	980	1800	Good wetting, but overly porous ceramic
22	Rosolite-Ta	49Ti-49Cu-2Be	980	1800	Good wetting, but overly porous ceramic, joint failed on cooling
23	Si_3N_4-Mo	49Ti-49Cu-2Be	980	1800	Excellent wetting, visible cracking of braze metal and ceramic
39	Platinized alumina[g]-Pt	49Ti-49Cu-2Be	980	1800	Excellent wetting, no cracks visible
40	Platinized alumina-Ir	49Ti-49Cu-2Be	980	1800	Excellent wetting, no cracks visible
43	Platinized alumina-Pt	72Ti-28Ni	1050	1920	Excellent wetting, no visible cracking
44	Platinized alumina-Ir	72Ti-28Ni	1050	1920	Excellent wetting, no visible cracking
45	Platinized alumina-Pt	48Ti-48Zr-4Be	1050	1920	Fair wetting

[a]All brazes in vacuum furnace at pressure of about 7 mPa (5×10^{-5} torr).

[b]Westinghouse designation for alloy of composition Fe–29% Ni–17% Co.

[c]Commercial nickel-clad titanium wire; all other filler metals were experimental powders, prepared by crushing cast buttons in a steel mortar and pestle.

[d]Rosolite ($Al_2O_3 \cdot 4SiO_2 \cdot 9Li_2O$) density was about 85% of theoretical.

[e]Cordierite ($2MgO \cdot 2Al_2O_3 \cdot 5SiO_2$) density was about 85% of theoretical.

[f]Silicon nitride density exceeded 90% of theoretical.

[g]Experimental material of alumina containing 0.5 vol % Pt.

molybdenum or tantalum was used for the base metal. Although we knew they could not be used in PKL, they were included to ensure the most advantageous stress conditions on the brazement. On the basis of this study we concluded that the alumina or platinized alumina ceramic joined to either platinum or Kovar with the experimental 49Ti-49Cu-2Be filler metal had the greatest chance of success from strictly a direct brazing standpoint for a ceramic-to-metal seal system. However, as was mentioned earlier, the thermal shock tests conducted about this time subsequently removed untreated Al_2O_3 from further consideration.

As can be inferred from our selection of metallic materials for the brazing tests, we had assumed from the very beginning of this program that we would be unable to braze the insulating material directly to the type 304L stainless steel because of the very high coefficient of expansion of that alloy. We intended to use one or more materials between the ceramic and stainless with the intermediate having a coefficient of expansion between that of the high-expansion type 304L stainless steel housing and the relatively low-expansion insulator. This technique is analagous to the "graded seals," which are used to join low-expansion glasses such as fused quartz to higher expansion glasses or to metals. We also intended to use the intermediate material as the electrode posts themselves. At this point the most likely candidate for the intermediate material was either Kovar or platinum.

As mentioned above we also conducted some brazing tests on ceramic materials that had been coated with either a moly-manganese or platinum layer. We encountered some difficulty with both coatings and ultimately both were at least temporarily dropped from consideration. Our problems with the moly-manganese coating were twofold. First there was the problem of application. Because of difficulties in locating a vendor who would rapidly coat small quantities of ceramic parts, we attempted to enter this difficult field of technology and coat our own components. After a number of unsuccessful attempts we were able to coat some of the ceramics with moly-manganese but were surprised to learn that when the proprietary slurry was fired at 1400°C (2550°F) in wet hydrogen there was undesirable reaction with several ceramics. Cordierite underwent significant erosion, rosolite evidently formed a low-melting glass, and the Si_3N_4 turned whitish-gray.

We were able to produce a tightly adherent moly-manganese coating on commercial Al_2O_3 or MgO disks, but then our second problem occurred — difficulties in brazing. A major concern whenever this coating is brazed is to use a filler metal (and heating time and temperature) such that the parts are wet and the joint filled but without dissolution of the coating.

In commercial practice the moly-manganese-coated ceramics are typically brazed with either the silver-copper eutectic alloy (BAg-8) or with pure copper or silver. All these filler metals are known to have poor resistance to corrosion by high-temperature steam and water. Some test specimens were brazed with the Au–18% Ni filler (BAu-4), which we knew had excellent corrosion resistance, but our results were not consistent. These inconsistent results were confirmed somewhat later when we did obtain and braze some commercially coated moly-manganese ceramics. We, therefore, had to abandon consideration of this technique as we did not have enough commercially coated ceramics or sufficient time to develop a consistent procedure.

During the early phase of our program we also investigated the use of a platinum sputtered coating on the ceramic material to promote wetting by a nonactive metal filler. Brazing filler metals were first selected on the basis of their potential for acceptable high-temperature steam corrosion resistance and/or high joint ductility and included the following: pure Au, BNi-2 (Ni-7Cr-4.5Si-3Fe-2B, %), BNi-4 (Ni-3.5Si-2B), and 62Cu-35Au-3Ni. In every case the brazing filler metal tended to dissolve the very thin (~5 μm) platinum coating and, therefore, not wet the cermet. To try to promote a more adherent or bonded layer of platinum on the platinized alumina cermets, we fired specimens in atmospheres of Ar–20% H_2 for 40 min at 1000°C (1830°F), 4 min at 1250°C (2280°F), and 3 min at 1500°C (2730°F). In the latter case the platinum layer appeared to have evaporated from the surface of the ceramic. In the other cases no observable effect was noted, but the ability of the coating to resist dissolution by the brazing filler metals was not enhanced.

After a number of attempts, several platinum-to-cermet subassemblies (in which the cermet had been coated with 5 μm of platinum) were successfully made with pure gold filler metal and brazing conditions of 5 min at 1070°C (1960°F). These parts, which were triaxial cable end seals as will

be discussed below, had acceptable helium leak rates after brazing but developed leaks after only one to five thermal shock tests. Since similar cable end seals directly brazed with the 49Ti-49Cu-2Be alloys were at that time capable of surviving 15 or more quenches, we decided to discontinue our efforts on the platinum sputtered cermets in order to concentrate on optimizing the direct brazing technique.

STEAM CORROSION TESTING OF BRAZED COMPONENTS

Inverted tee specimens of type 304L stainless steel joined to either platinum or Kovar sheet by various brazing filler metals were exposed to high-temperature steam with the following accumulated time-temperature conditions:

(1)	900°C (1650°F) 0.5 h	(6)	600→500°C (1110→930°F) 1.5 h
(2)	900→800°C (1650→1470°F) 5 h	(7)	500→400°C (930→750°F) 1 h
(3)	800→700°C (1470→1290°F) 2 h	(8)	400→300°C (750→570°F) 1 h
(4)	700°C (1290°F) 3 h	(9)	300→200°C (570→390°F) 1 h
(5)	700→600°C (1290→1110°F) 6 h	(10)	200→100°C (390→210°F) 12 h

The tests were conducted in a test loop, which heated plant steam by passing through a section of nickel alloy tubing electrically heated by its own resistance. Unfortunately the purity of the steam in this system was never determined, so the information obtained was only qualitative. What we did do was to metallographically compare the effect of the exposure on a given braze alloy with the effect on the type 304L stainless steel as would be used in the PKL test bundle. Photomicrographs of some of the samples before and after exposure are given in Figs. 10 and 11. The unexpected results from this study was the good corrosion resistance of the 49Ti-49Cu-2Be experimental filler metal, which appeared to corrode to about the same extent as the stainless steel. Note also that the fillet of the commercial nickel-titanium alloy (also a direct braze material) has been completely corroded by the steam. We were also concerned by the cracking that occurred in the fillet of the Kovar-to-type 304L specimen [Fig. 11(c)], which was brazed with 49Ti-49Cu-2Be. This observation, along with the grain boundary corrosion in the Kovar (Fig. 12) led us to select platinum rather than Kovar as the transition material.

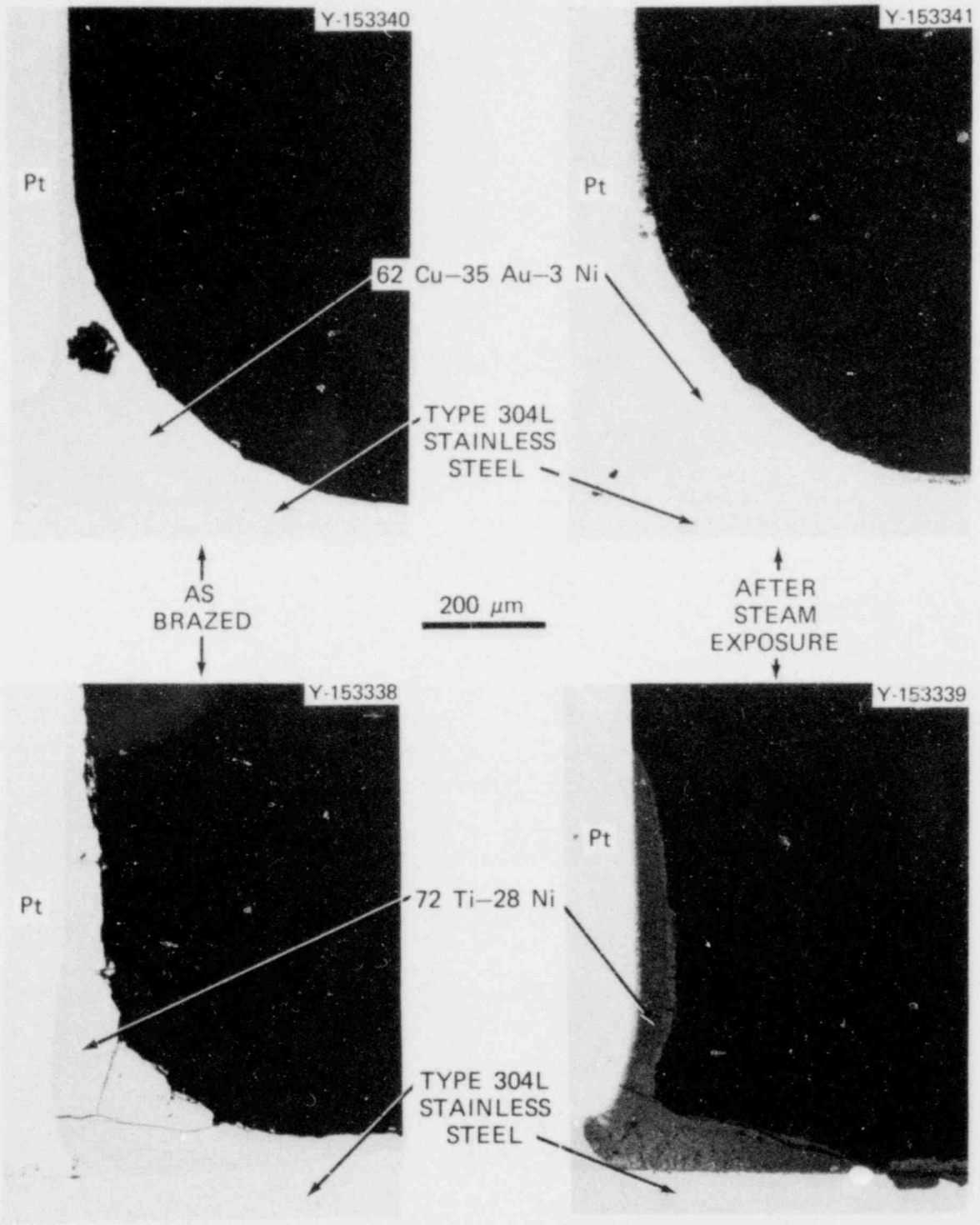

Fig. 10. Inverted Tee Braze Specimens of Platinum to Type 304L Stainless Steel Both as Brazed and After High-Temperature Steam Exposure (See Text for Temperatures). Unetched.

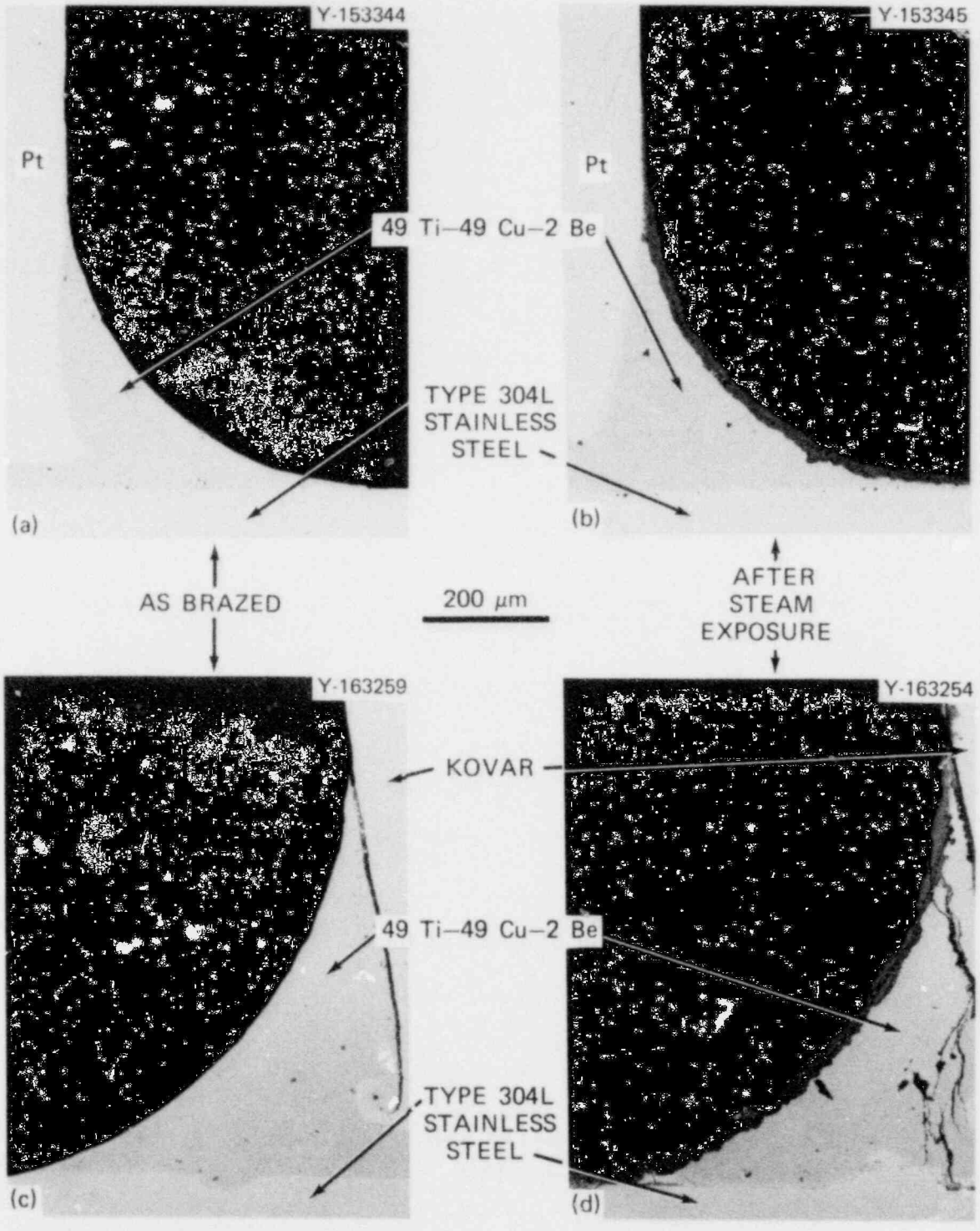

Fig. 11. Specimens of Platinum and Kovar Brazed to Type 304L Stainless Steel with 49Ti-49Cu-2Be Filler Metal Both as Brazed and After Exposure to High-Temperature Steam. The cracks in the fillet in (c) and (d) are apparently the result of the large difference in coefficients of thermal expansion of the Kovar and stainless steel.

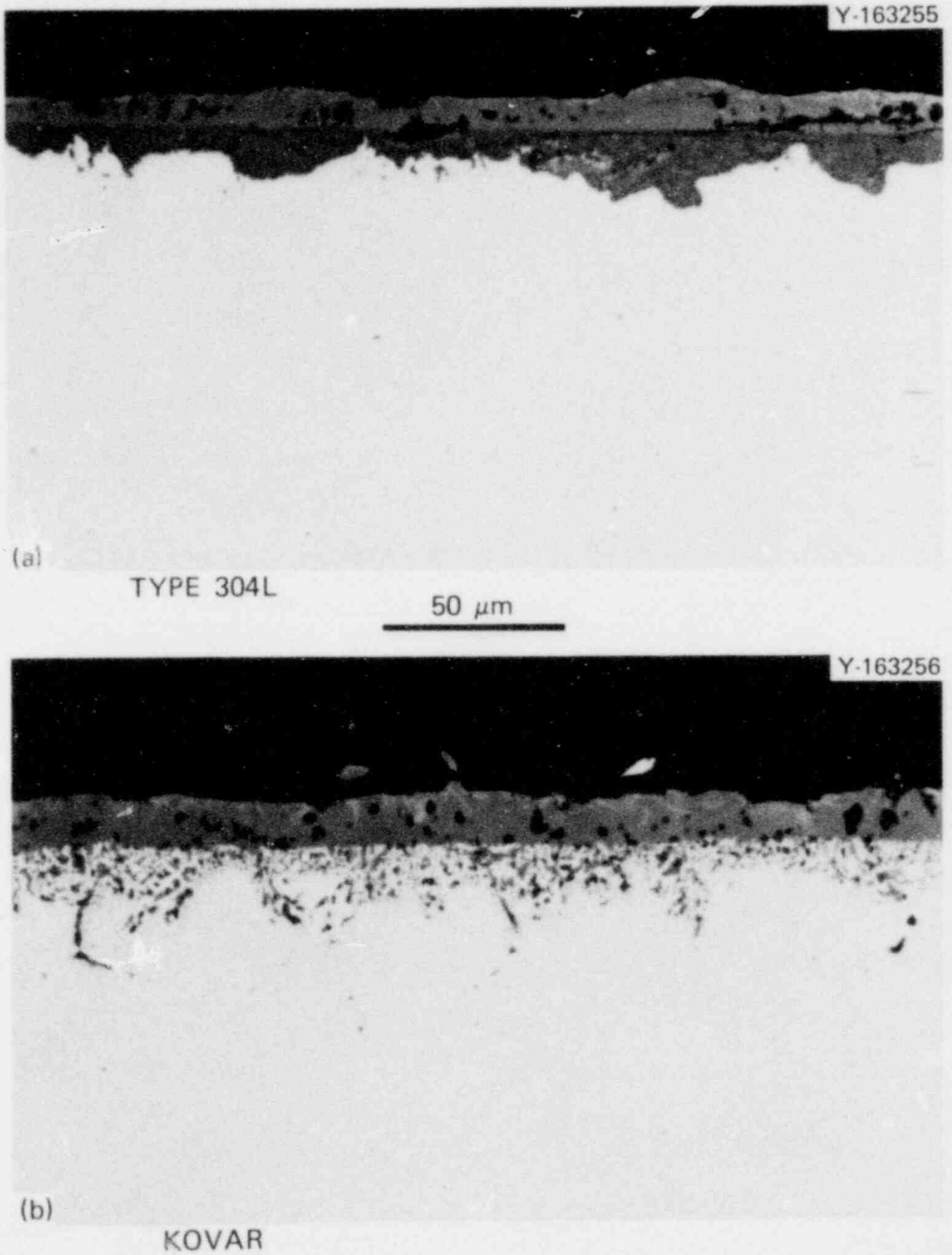

Fig. 12. Comparison of the Corrosion of (a) Type 304L Stainless Steel and (b) Kovar When Exposed to High-Temperature [800–900°C (1470–1650°F) steam (see text for details of exposure). As polished.

Thus, for the sensors for PKL, we selected a ceramic-to-metal seal system that consisted of a platinized alumina cermet insulator brazed to a platinum transition material with a filler metal of 49Ti-49Cu-2Be. How this general concept was applied to the actual components themselves will

be discussed below. In addition several other difficult braze joints and our techniques for joining them will also be covered.

FABRICATION OF INSTRUMENTED RODS

Cable End Seal Fabrication

The design for the seal that was used on the sensor end of each of the eight 3.18-mm-diam (0.125-in.) triaxial cables of each instrumented rod is shown in Fig. 13. The purpose of this seal was to prevent

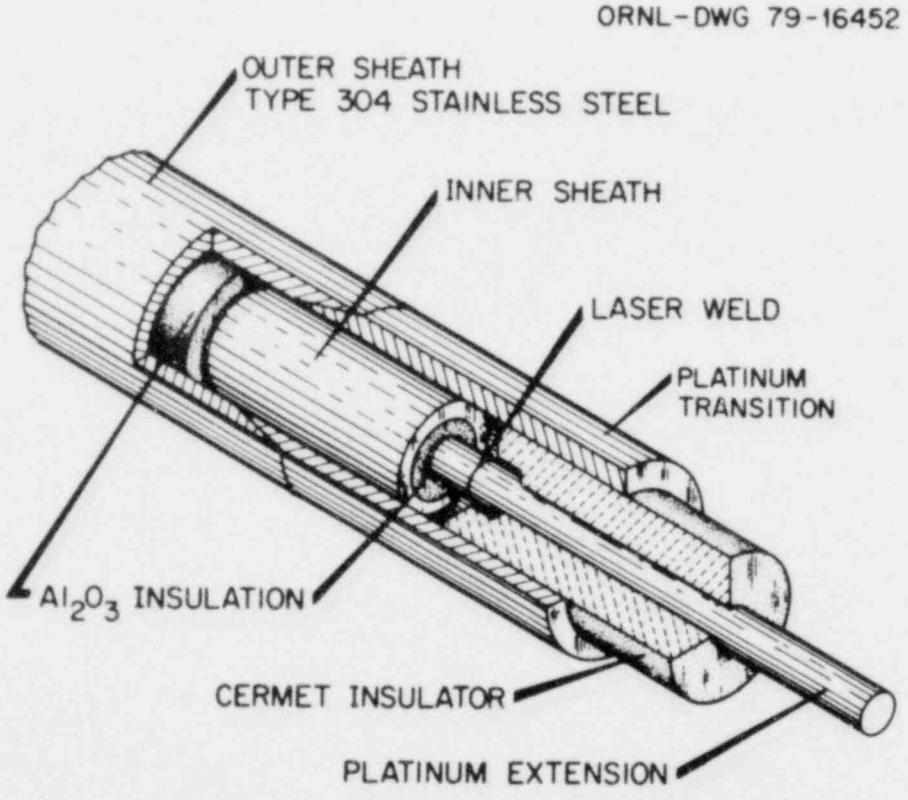

Fig. 13. Design of End Seal for 3.18-mm-diam (0.125-in.) Stainless Steel Triaxial Cable.

moisture from being absorbed in the insulation of the cable thereby changing the electrical signals from the sensors. We were concerned both about moisture from the atmosphere (so that the instrument end of the leads was sealed with epoxy) and with steam or water that might penetrate

the rod during testing. Electrical checks on lengths of cables that had been intentionally wet with water showed that a sensor was capable of functioning unless the cable was wet with the amount of water equivalent to a room-temperature helium leak rate of 4 mm^3/s. Although cable end seals that leaked at any rate less than this would therefore be expected to remain functional, we maintained a leak rate standard of less than 1×10^{-5} mm^3/s for all the cables for the PKL instruments. The second major requirement for the cable was an electrical resistance between the three conductors (outer sheath, inner sheath, and central wire) of about 1 MΩ or greater, and capacitance (C) values of $\geq 0.52L$ $(0.16L)$ nF [where L is length of cable in meters (feet)], and loss factor less than $\sqrt{(0.52L/C)^2 - 1}$.

A notable feature of the design is the tapered joint between the platinum transition and the outer sheath of the cable. Because of the limited space inside the stainless steel tube, the outside diameter of the transition joints could be no larger than that of the cable itself. Thus an external socket joint was not possible. Also the close proximity of the inner sheath eliminated some other joint possibilities. As an overlapping rather than a butt joint was necessary to obtain an adequate braze area for strength and sealing, we had the choice of either a step joint or the tapered lap. We selected the latter primarily because we had been having good success with this configuration in brazing of thin-wall tubular conductors for another program.[9] Besides providing a relatively large braze faying surface, this joint is self-aligning and so requires no fixturing. Note that the stainless steel (which has a higher coefficient of expansion than the platinum) is made the external or female member of the joint. Thus, on cooling from the brazing temperature, the joint is put in compression by the contracting stainless steel cable.

Another important feature of the design was the transition from the 0.69-mm-diam (0.027-in.) stainless steel central conductor to a 0.51-mm-diam (0.020-in.) platinum wire, which passed through the cermet insulator, as can be seen in Fig. 14. This transition, which was accomplished by a pulsed ruby laser weld joining the butted wires, was necessary to avoid damage to the tightly fitting insulator at the brazing temperature due to the thermal expansion mismatch. An alternative technique would have been

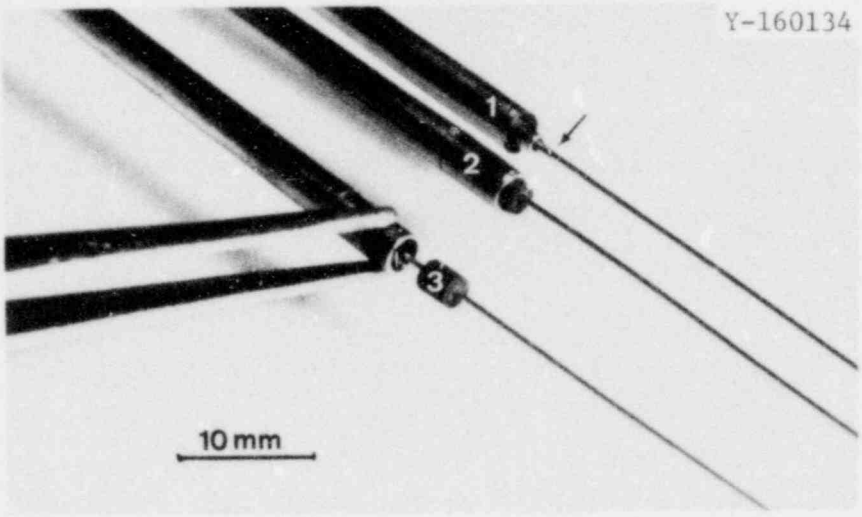

Fig. 14. Assembly of Components for a Cable End Seal in Preparation for Brazing. 1, 3.18-mm-diam stainless steel cable, showing end preparation (laser weld of platinum extension is indicated by an arrow). 2, Platinum transition. 3, Cermet insulator.

to fit the stainless steel conductor and cermet loosely at room temperature so that expansion on subsequent heating would give the tight fit required for brazing. However, on cooldown the wire would contract considerably more than the insulator, putting the braze joint and ceramic in tension, an undesirable condition.

The two criteria for the cable end seal, leak tightness, and high electrical resistance, led to conflicts when we began brazing cables. The way to ensure that a braze joint is leaktight is normally to apply an abundance of brazing filler metal to the joint, and this is particularly true in dissimilar-material joining, where the brazing gap generally increases on heating. However, in this case unless the amount of alloy was very closely controlled the molten metal flowed completely through the joints on the cermet and electrically shorted out the seal internally. Although the alloy also generally wet the entire external end of the cermet thereby shorting the central conductor to the platinum transition and outer sheath (Fig. 15.), this could be and was routinely remedied after brazing by manually beveling the corner of the insulator with an abrasive stone to reveal bare cermet. In the case of an internal short there was no remedy, so that the defective seal had to be cut off and the cable end remachined. The internal shorting problem was effectively controlled, but

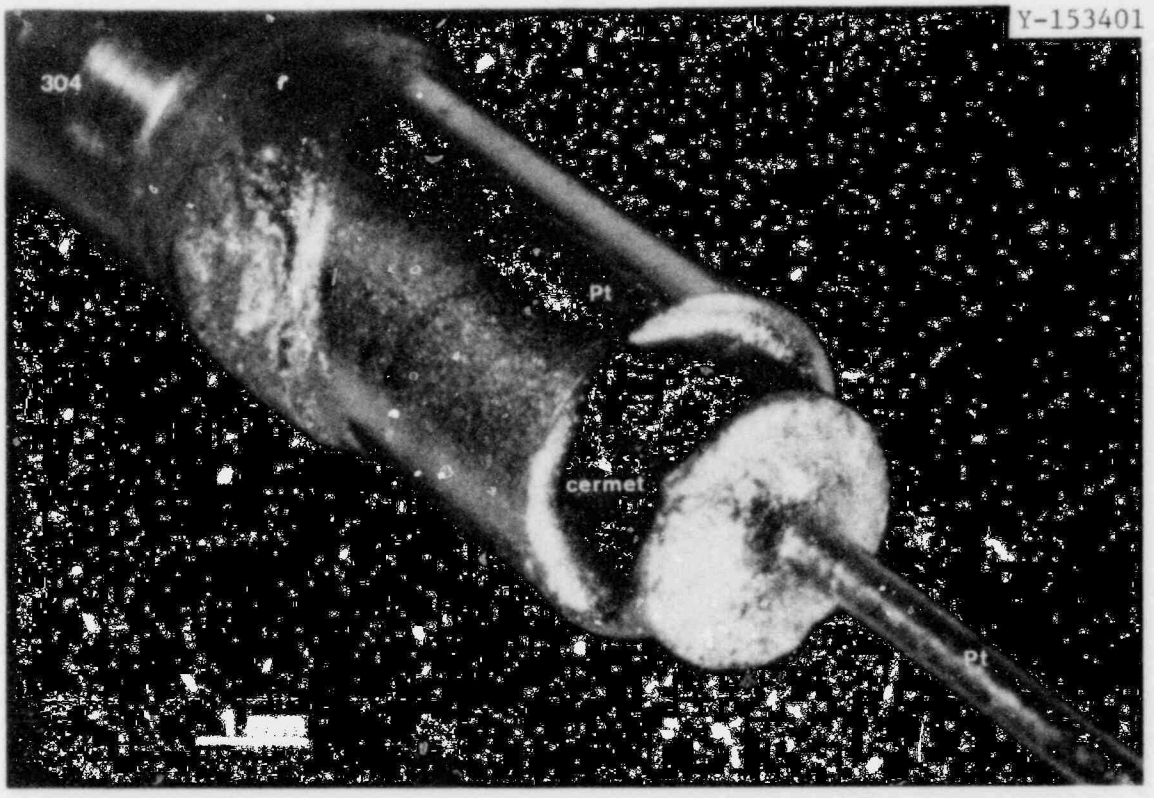

Fig. 15. Cable End Seal After Brazing With a Direct Brazing Filler Metal (49Ti-49Cu-2Be).

not entirely eliminated, by (1) keeping the amount of filler metal powder preplaced at the joint areas to a minimum, (2) keeping the brazing temperature low and the time at temperature short to minimize alloy flow, and (3) counterboring the cermet on the inside to provide a dam to limit capillary flow.

A resistance-heated vacuum furnace (Fig. 16) having a 51-mm-ID by 2.13-m-long (2.0 × 84 in.) ceramic tube was used in brazing the end seals to all the triaxial cables. Because the length of the cables ranged up to 7.9 m (26 ft), it was necessary to extend the excess out through the end of the furnace tube. This was accomplished by passing each cable (of a batch of five brazed at a time) through a hole in a large rubber stopper. The joint between the cables and stopper was subsequently sealed with a compound made for that purpose so that the tube could be evacuated to about

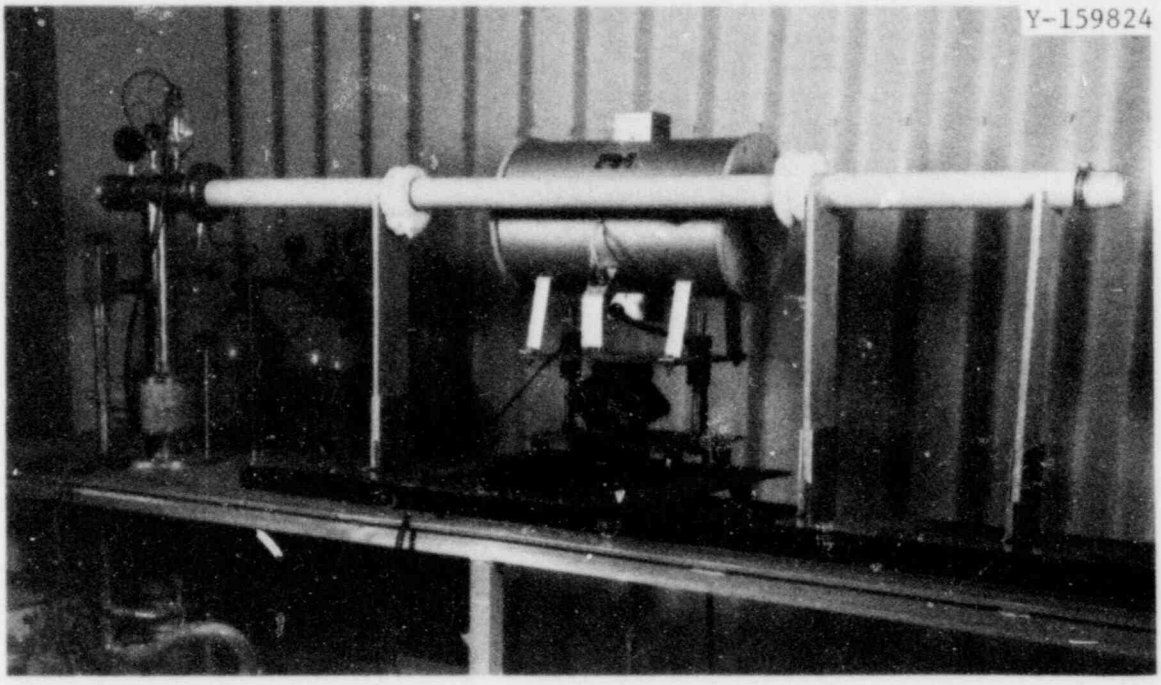

Fig. 16. Vacuum Furnace Used to Braze the Cable End Seals in Batches of Five. The cables extend out through the tube support at left during brazing.

13 mPa (1×10^{-4} torr). We found it necessary to bake out the cable ends by heating in the same furnace for 15 min at 980°C (1800°F) to remove gases and moisture before assembly and brazing. After bakeout the end seals were assembled, the 49Ti-49Cu-2Be filler metal powder was applied, and the heating element was moved around the furnace tube until a thermocouple near the parts reached 930°C (1710°F). Then the furnace was lowered and rolled back. We also washed the cermets in acetone and then fired for 15 min in air at 800°C (1470°F) before assembly for brazing to remove any contaminents (such as machining lubricants) from the surface.

After brazing each end seal was given a preliminary leak test by pressurizing externally with 0.34 MPa gage (50 psig) of helium for 30 s and then quickly removing the pressurization fixture and immersing the brazement in alcohol. The absence of bubbles in this test indicated a probable leak rate of less than 1×10^{-3} mm^3/s (as shown by a calibration test with a glass capillary) so that the excess filler metal could be removed to isolate the central conductor before the electrical tests and

the final leak check with the mass spectrometer. If one or more areas were leaking, additional filler metal powder mixed with an acrylic binder was added and the cable was rebrazed, again heating to 930°C (1710°F).

The final leak check consisted of pressurizing the seal area in a small fixture at a pressure of 0.41 MPa gage (60 psig) of helium and holding for 10 min to allow helium to penetrate any leak. Then the pressurization fitting was quickly removed and the part connected to the mass spectrometer.

During the course of this program over a hundred triaxial cables were sealed with a cermet insulator by using the technique described above. Five samples, selected at random, were given 50 thermal shock tests from 520°C (970°F) air into 80°C (175°C) hot water and then inspected by pressurizing the short lengths of cables with helium at 0.17 MPa gage (25 psig) and immersing in alcohol, with the following results:

1. After five quenches no seals leaked.

2. After ten quenches one seal had a small stream of bubbles emanating from the platinum-wire-to-cermet joint.

3. After 20 quenches two samples had a small stream of bubbles from around the wires.

4. After 30 quenches no leaks were observed.

5. After 50 quenches the seal that leaked after 10 quenches now leaked again.

The quenched seals were subsequently leak tested by using the helium mass spectrometer, and two had leak rates less than 1×10^{-7} mm^3/s, one a rate of 2×10^{-4}, and two "gross" leaks. Evidently one of these had a leak rate just detectable by the immersion method (as we learned on rechecking) but relatively large by the leak detector sensitivity. Thus, we feel confident that an end seal in a rod tested at PKL (where the thermal transients inside the tube should be much less severe) is very unlikely to develop a leak rate greater than the maximum allowable of 4 mm^3/s.

Sensor Subassembly Fabrication

The evolution of the sensor portion of the instrumented rod is shown in Fig. 17. The first prototypes were flat rather than curved because

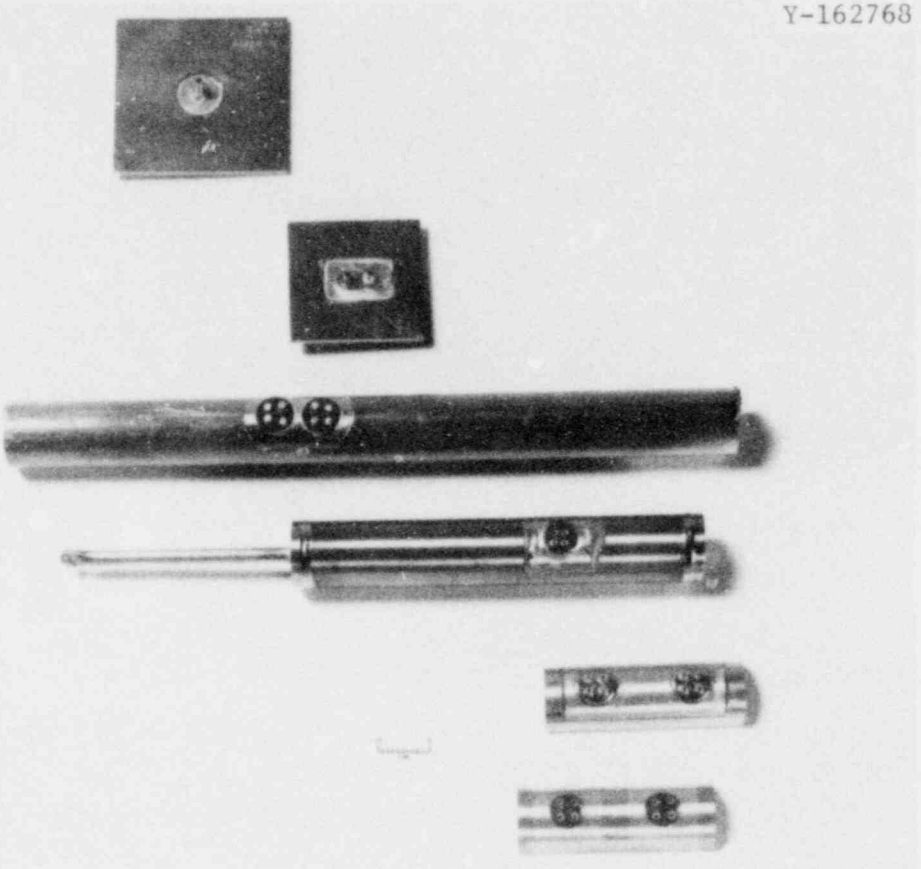

Fig. 17. Various Steps (top to bottom) in the Development of the Impedance Probe Sensor Module With the Final Design of a Flag Probe Subassembly at the Bottom.

materials were more readily available in that geometry and we also wanted to minimize machining problems to expedite development of the seal. The other stages of the development were prompted by changes in electrode spacing by the instrument designers and to improve fabricability and integrity of the sensor. Since they help to explain how the final design was arrived at, each of the evolutionary stages will be discussed in some detail below.

The component parts that constituted the first step in sensor development are shown in Fig. 18. The use of a tapered platinum bushing was based on our thinking that it would move further into the stainless steel housing during brazing and therefore maintain intimate contact in spite of the mismatch of coefficient of thermal expansion. A thin filler metal

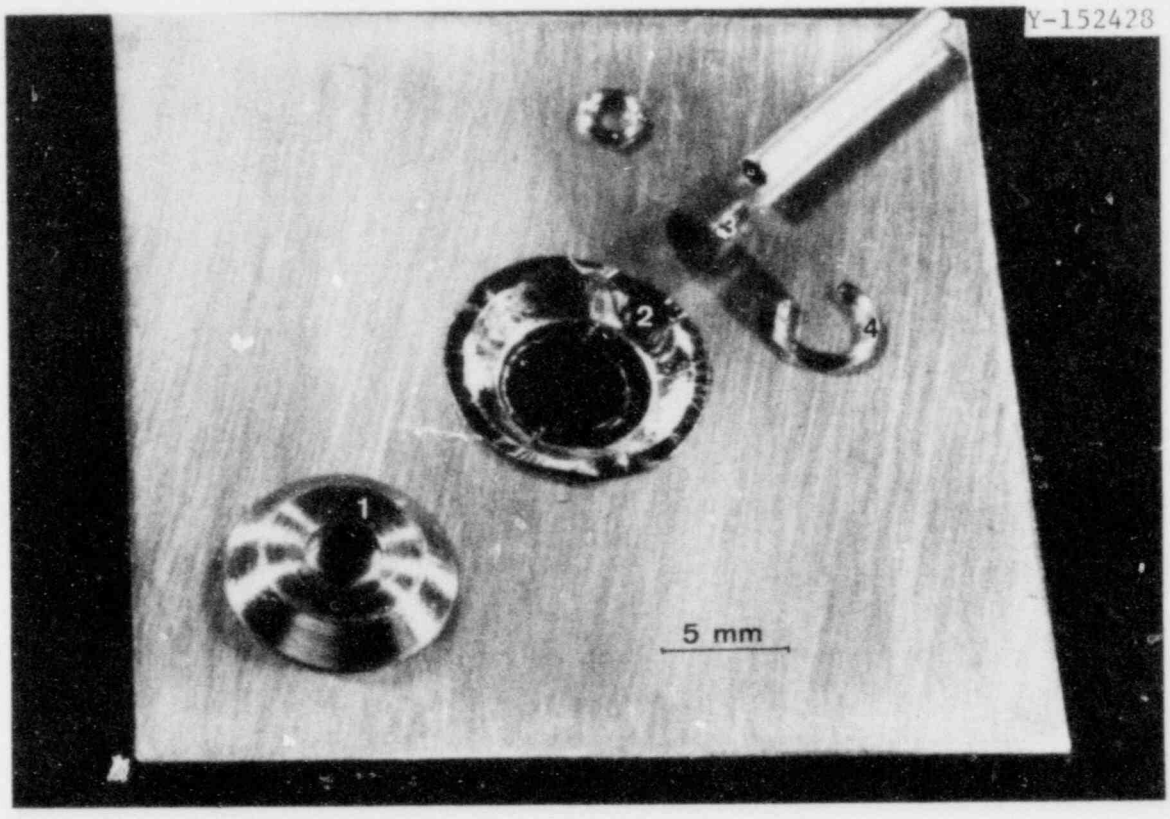

Fig. 18. Components for Initial Development of a Sensor Subassembly. 1, Platinum bushing. 2, Pure gold foil filler metal. 3, Platinized alumina cermet. 4, Nickel-clad titanium filler metal ring.

shim of pure gold was preplaced at the faying surface between the platinum bushing and stainless steel, and rings of commercial nickel-clad titanium alloy (72Ti-28Ni) were used to braze the cermet both to the bushing and to a platinum tube representing a plug that would support a sensor electrode. The platinized alumina cermets being made at that time had densities about 90% of theoretical. The part was brazed in the tubular vacuum furnace in Fig. 19, being held at 1070°C (1960°F) for 10 min. Although we were unable to leak-test parts of this design because of the platinum tube, we were encouraged because no cracks were visible in the cermet after brazing. A poorly designed metal-to-ceramic seal will generally fail during this first thermal cycle between brazing and room temperature. Two of these parts (one of which is shown in Fig. 20) were tested for thermal shock resistance by heating to temperature in air and then dropping into water at 80°C (175°F). The first assembly was heated to 600°C (1110°F) and had visible

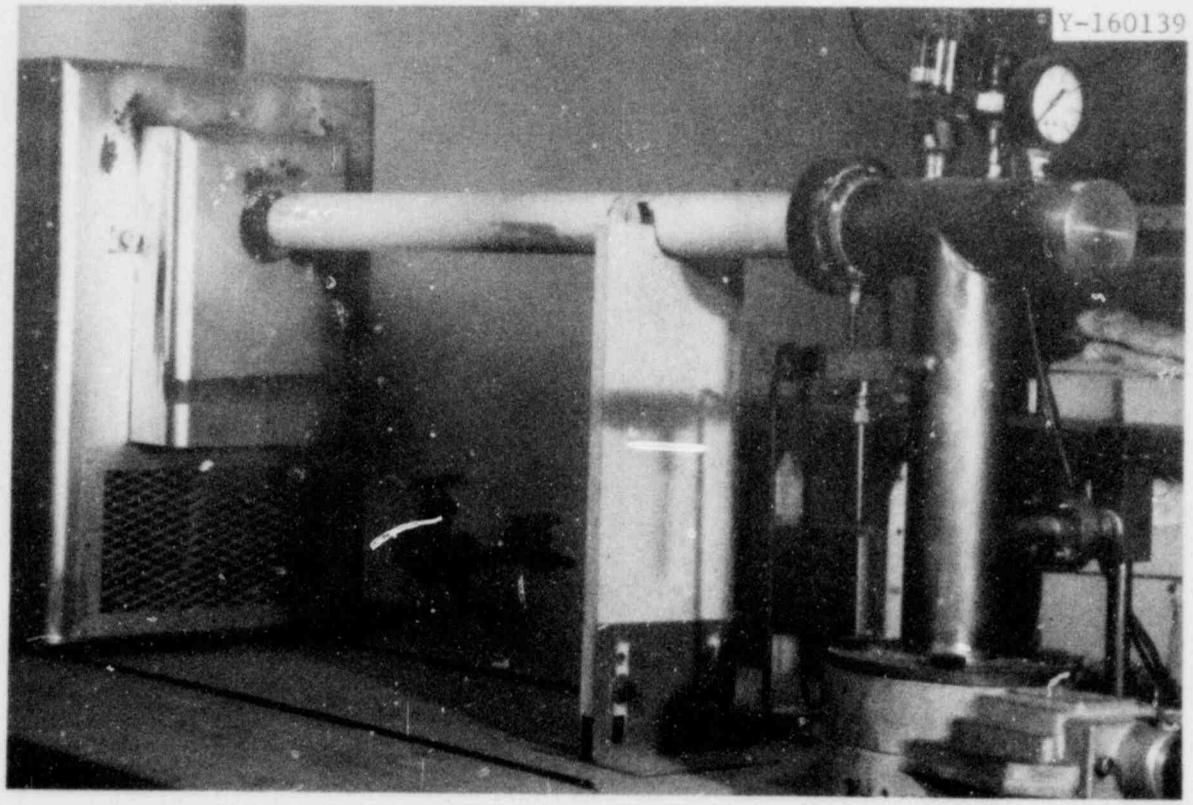

Fig. 19. Tubular Vacuum Furnace Used to Braze Sensor Subassemblies. The preheated unit at left, with SiC elements is rolled to the right to surround the mullite tube containing the components in a molybdenum foil boat.

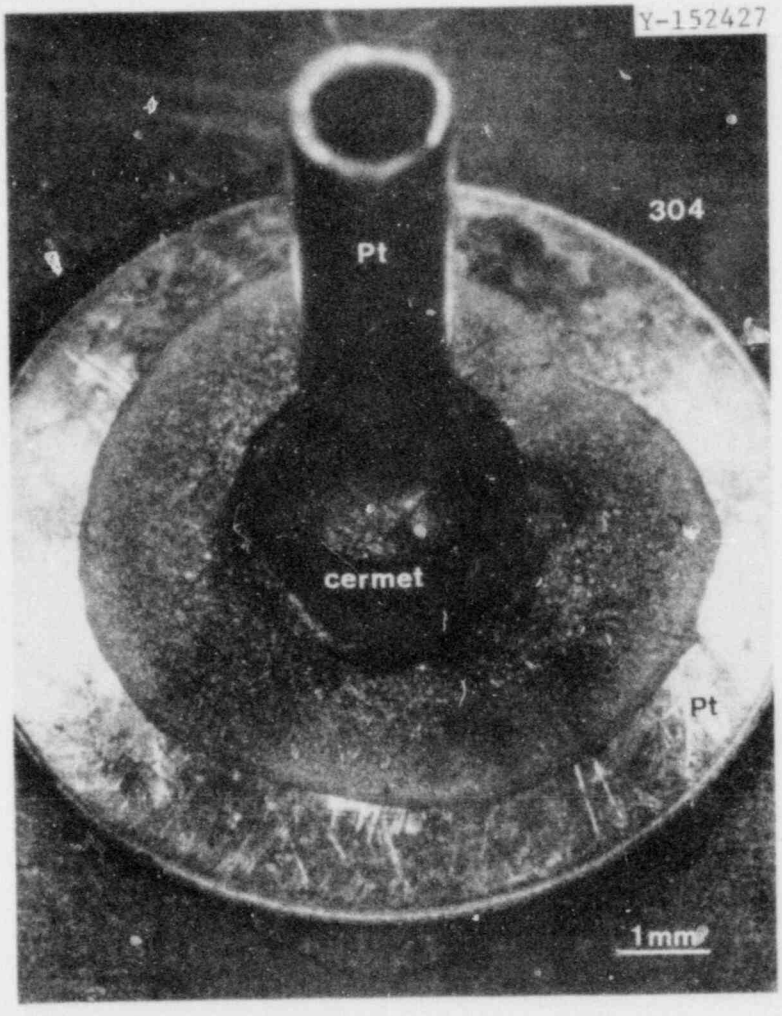

Fig. 20. One of the First Sensor Subassembly Development Test Pieces After Brazing with Nickel-Clad Titanium (72Ti-28Ni) Filler Metal.

cracking on the underside after the third cycle. The second part had no cracks visible at a magnification of 30× after ten quenches from 520°C (970°F) air.

Because of the favorable results with the single cermet assembly, the dual insulator component shown in Fig. 21 was brazed, again by using gold foil and nickel-clad titanium filler metals and a temperature of 1070°C (1960°F) for 10 min. The fitup between the platinum transition and the type 304L stainless steel housing was poor because of difficulties in machining, so that the resulting braze at that joint was not continuous, particularly at the corners. There was thought to be enough braze, however, to transmit the stresses such that a valid thermal shock test could be conducted. The

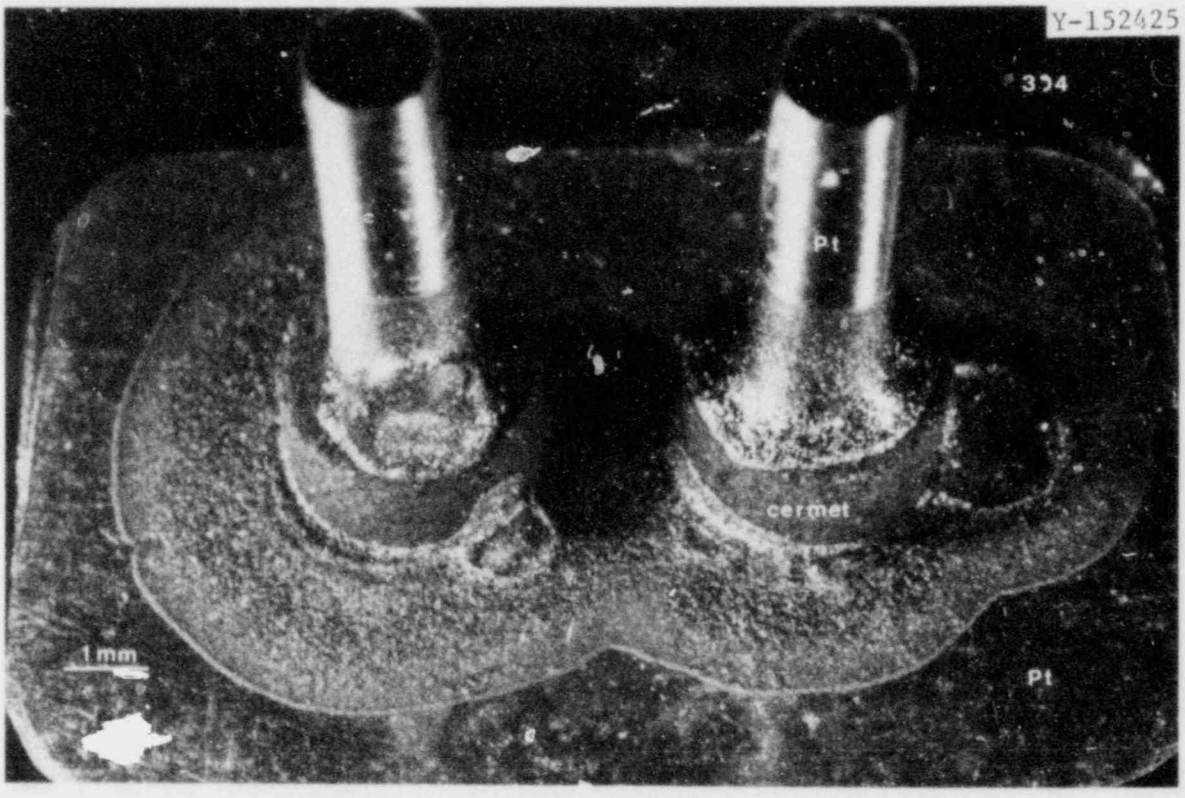

Fig. 21. Second Step in Sensor Subassembly Development with Two Cermet-to-Metal Seals. Again the filler metals were gold foil (platinum to type 304L stainless steel) and nickel-clad titanium (ceramic to platinum bushing and tubes).

part was quenched from 520°C (970°F), and no cracks were detected until after the seventh cycle. Then one cermet was cracked on the underside.

In order to verify these excellent thermal shock test results on a more prototypic specimen, the first of the components having a curved platinum transition piece was designed and fabricated (Fig. 22). The upper part in this figure was made in the configuration of the prong probe sensor design at that time and therefore had two 3.25-mm-diam (0.128-in.) single-hole cermets with a center-to-center spacing of 4.78 mm (0.188 in.) Two assemblies of this type, in which the cermet insulators were coated with 5 μm of platinum, were brazed by using pure gold as the filler metal. In both cases the joint between the platinum transition piece and the stainless steel tube leaked badly after brazing. In one unit the cermet-to-platinum-plug joints also leaked badly, but in the other all the brazes

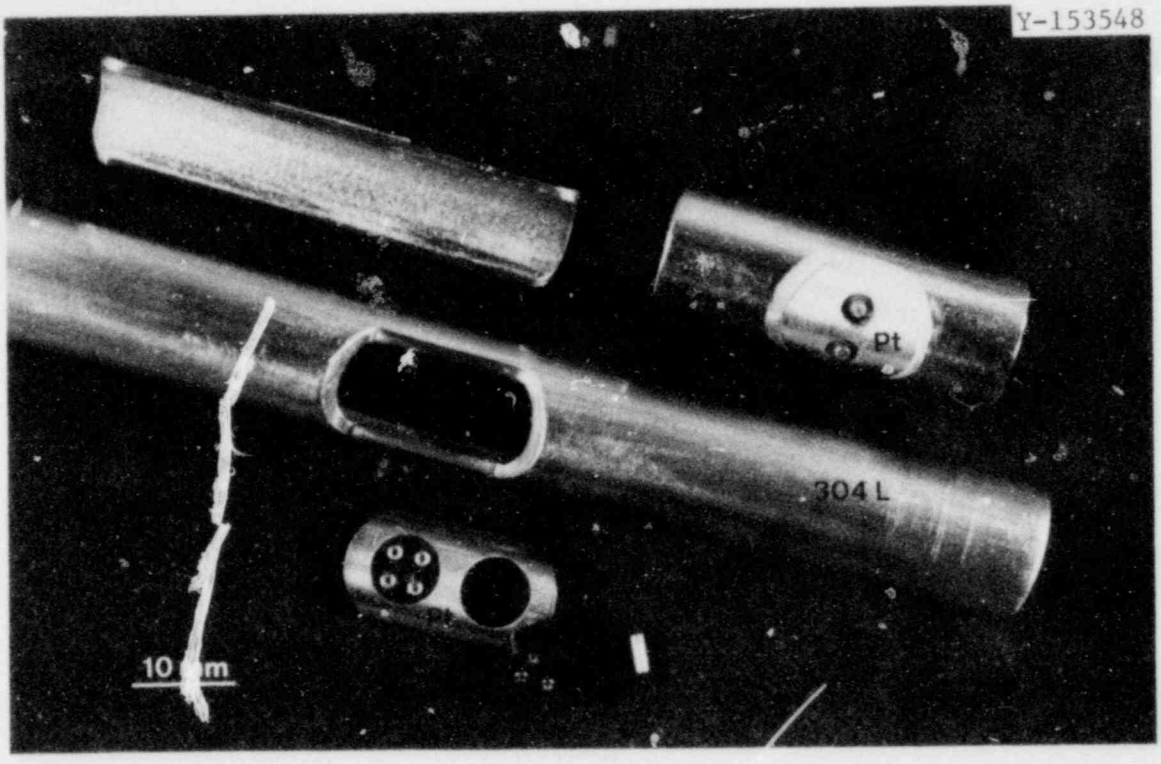

Fig. 22. First Sensor Subassembly Prototype with Curved Geometry (upper right), and Flag Probe Module with Four-Hole Cermets on a 9.53-mm (0.375-in.) Center-to-Center Spacing. The cover for the access opening behind the sensor braze area is at upper left.

between the insulators and platinum were leaktight as determined by pressurizing the tube with 69 MPa gage (10 psig) helium and immersing in alcohol.

The lower set of components in Fig. 22 was for a slightly later design for a flag probe subassembly. At that time the spacing between sensors had been decreased to the final dimension of 3.05 mm (0.120 in.). Thus there was no longer space for individual insulator bushings, and these were replaced by two four-hole ceramics in the case of a flag probe sensor. Note that the center-to-center spacing between the groups of four electrodes was 9.52 mm (0.375 in.) and not 19.05 mm (0.750 in.), which was eventually used.

We were unsuccessful in brazing assemblies of this design because of continuing problems at the joints between the platinum transition and the type 304L stainless steel tube. This beveled geometry on the platinum to stainless joint was used to conform as closely as possible to the highly

successful tapered platinum bushing in the early flat assemblies (Fig. 18). However, we were never able to machine this joint with a tight enough fit for brazing, particularly in view of the mismatch in coefficients of thermal expansion of the two materials.

We subsequently modified our design to that of the platinum transition with square ends (rather than beveled at 45°) shown in Fig. 23.

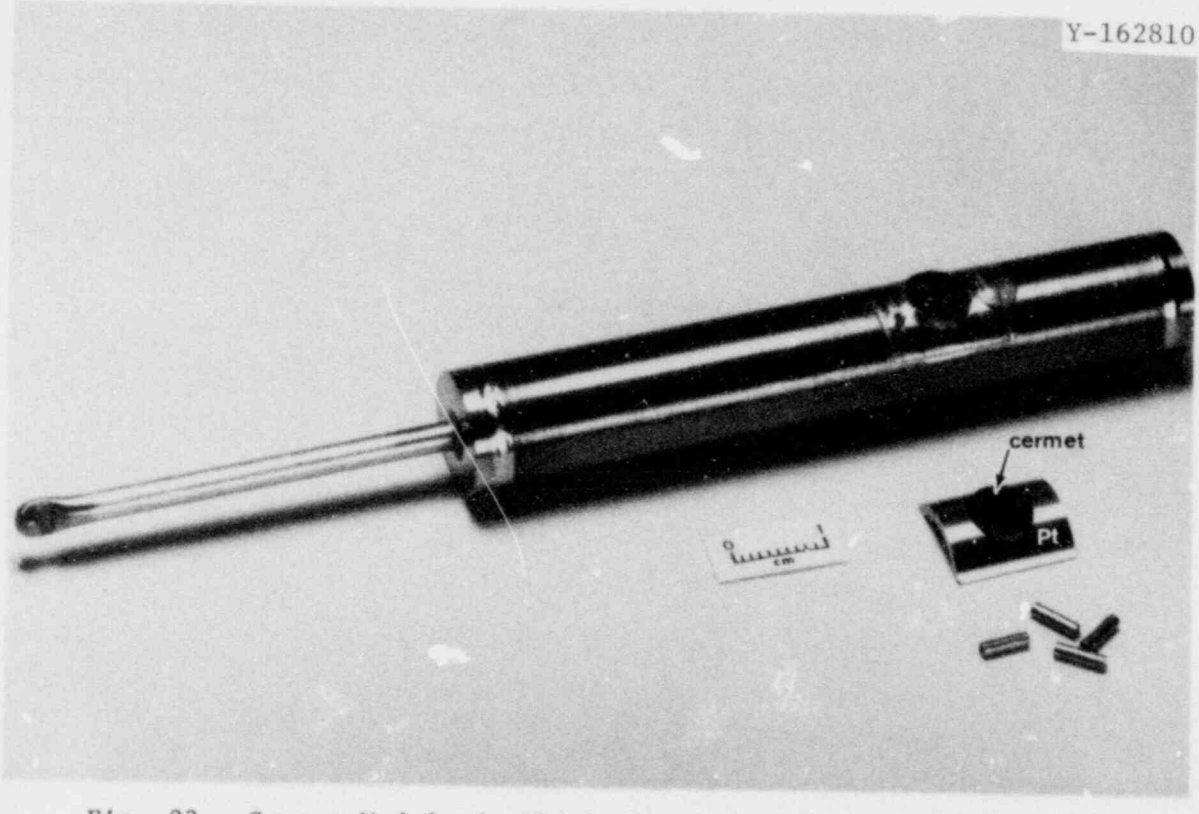

Fig. 23. Sensor Module in Which the Platinum Transition Fits in a Rectangular (Rather than Beveled) Opening in the Guide Tube Wall.

This model was very successful and geometrically was the forerunner of the type of sensor subassembly that was eventually installed in the rods for PKL. Several of these units were brazed by using the experimental 49Ti-49Cu-2Be filler metal powder at the ceramic-to-platinum joints and BAu-4 (Au-18% Ni) wire to join the platinum transition piece to the tubing. Two of these assemblies were given a series of thermal shock tests from 520°C (970°F) air into hot water. In the first, no bubbles were observed in the helium pressurization [0.17 MPa gage (25 psig)] alcohol immersion test after five quenches, but two streams of tiny bubbles were noted after ten cycles.

The second part was quenched 30 times and subsequently had three very small helium leaks. During this series of tests we first observed a phenomenon that we have noted several times since. This is the sealing of leaks (microcracks) in the platinized alumina cermet materials as the result of interaction with hot water. Thus, during the series of 30 thermal shock tests we noticed that a leak would appear but then be gone after several more exposures. We assume that this phenomenon was due to the formation of a hydrate in the insulator material and would be beneficial in healing leaks in a sensor exposed to hot water and steam.

Although these results were instrumental in finalizing the general design of the ceramic-to-metal seal system for the prong and flag probes, several significant changes were made before this phase of the AIRS program was completed with the shipment of six instrumented rods to Germany. The first change dealt with the basic idea of just how and when the sensors would be installed in the 4.32-m-long (170-in.) tubes. Originally we had planned to braze the sensor module (platinum transition, cermet, and plugs) directly into the rod, attach the electrical leads by way of a hole in the tube wall, and then weld a cover over this opening. Note, for instance, in the upper left of Fig. 22 an access window cover, which was to have been welded into the tube after the wires from the triaxial cables had been joined to the inner end of the platinum plugs. This concept was abandoned for several reasons. First, we realized that our success rate in brazing these complex seal assemblies with their many joint areas was not very high, and that if a given leaking sensor assembly was not repaired even after rebrazing, we would eventually have to scrap a complete rod. This would be true even if the sensors at another level were fully acceptable. Second, we anticipated difficulties in brazing sensor modules into a tube of this length while sealing all the various openings to maintain a sufficiently high vacuum for the Ti-Cu-Be filler metal. And, finally, we realized that the machining operation to remove the excess brazing filler metal, which flows over both the inner and outer surfaces of the cermet (thereby shorting all the sensor plugs together), would be very difficult from access and handling standpoints if the insulators were attached to 4.3-m-long tubes.

We avoided these potential problems by changing to a concept in which the sensors were fabricated in subassemblies that could be machined and inspected for leaktightness and electrical properties before being joined to the guide tube. Each subassembly was made up of cermet insulators, platinum electrode support plugs, a platinum transition piece, and a stainless steel frame. The modules are small enough to be brazed in the small vacuum furnaces of the type shown in Fig. 19, and the subsequent final machining and inspection operations are relatively simple. As can be seen in Fig. 24, we also eliminated the access opening behind each sensor location and instead elected to have one opening machined into the tube at each level. This figure shows two flag probe subassemblies with the part shown welded into the tube being of the old design with 9.52 mm (0.375 in.) spacing between groups of electrodes.

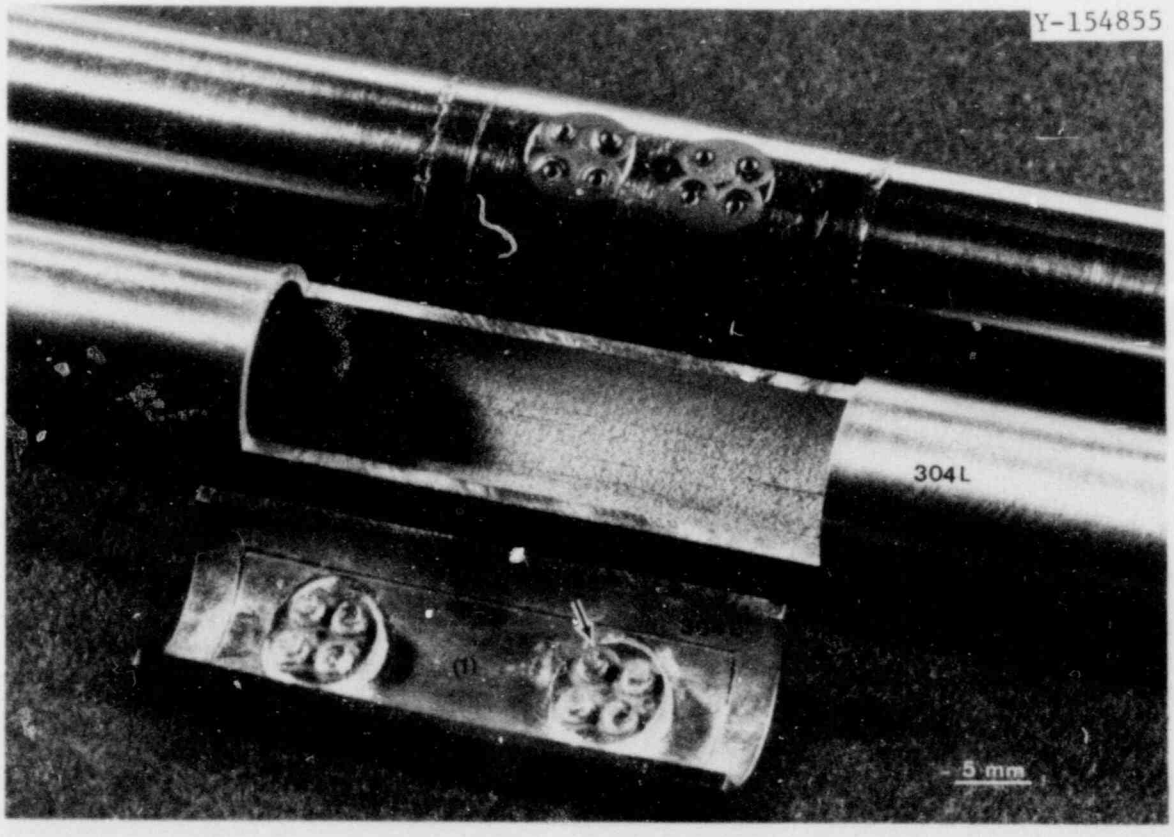

Fig. 24. Prototypic Flag Probe Impedance Sensor Subassembly Before and After Being Laser Welded into the Stainless Steel Housing. Parts of this design, with a single platinum transition piece (1), were included in the instrumented rods shipped to Germany. Note the core-drilled areas around each of the platinum plugs (arrow).

The modules are joined to the tube by using a pulsed ruby laser welder and a series of overlapping spot welds to make a helium-leaktight joint. We had considered carefully controlled, low-heat-input gas tungsten-arc welding and electron beam welding for welding in the access window cover in the earlier concept. However, the tubing showed unacceptable amounts of distortion, so these processes were not considered for welding in the sensor modules. The pulsed laser process, by its intermittent nature and low total energy input per pulse, also eliminates overheating the adjacent braze joints during welding. Both the edge of the opening and the sensor subassembly are beveled slightly to accept a piece of 0.25-mm-diam (0.010-in.) type 308 stainless steel filler wire to reduce the probability of weld hot cracking. These welds are inspected for leakage while still at the laser console by pressurizing the rod with 0.17 MPa gage (25 psig) helium and immersing the sensor area in alcohol through use of a glass envelope sealed with rubber stoppers slid over the tube. Thus any leaks can be detected and repaired without having to transport the rod to and from an inspection station.

Figure 25 depicts a flag probe sensor array installed in a guide tube by the subassembly technique. Note that the leads from the triaxial

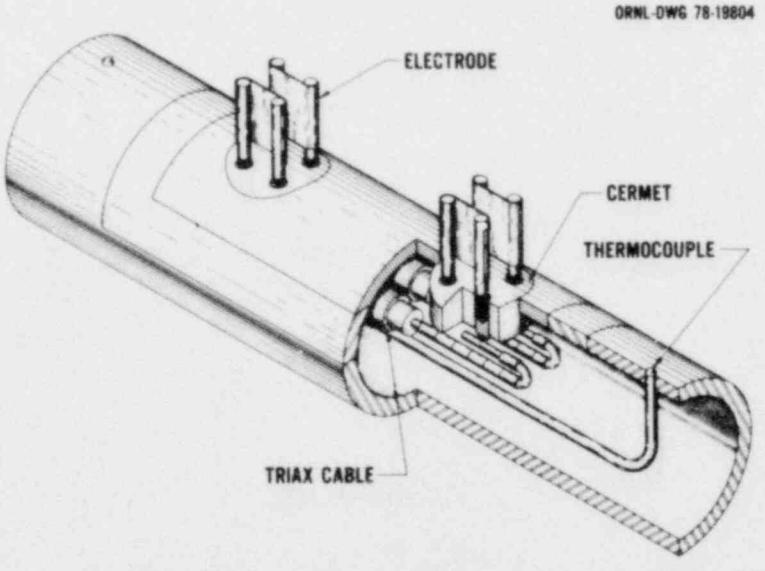

Fig. 25. Flag Probe Subassembly and Thermocouples Installed in a Guide Tube Rod. The design shows a single platinum transition piece containing two four-hole cermet insulators. Pt–30% Rh was used as the electrode (flag) material.

cables are bent in a loop to allow some flexibility as the module is pushed back into the opening for the closure. The 0.51-mm-diam (0.020-in.) wires are encased in thin-walled alumina insulator tubing to prevent short circuits during testing. As mentioned earlier, the platinum leads are joined to the inside of the sensor support plugs by using the pulsed laser welder. This drawing is somewhat misleading in that it only portrays a sensor array at the lower elevation in a rod. At the upper level sensor, the available space is much more limited because the four 3.18-mm-diam (0.125-in.) cables and two 1.02-mm-diam (0.040-in.) thermocouples for the lower level must also be accommodated in the 11.23-mm (0.442-in.) bore of the tube.

Joining of Thermocouples to Instrumented Rod

The two stainless-steel-sheathed thermocouples at both sensor locations in a rod were attached by induction brazing (Fig. 26) in a helium

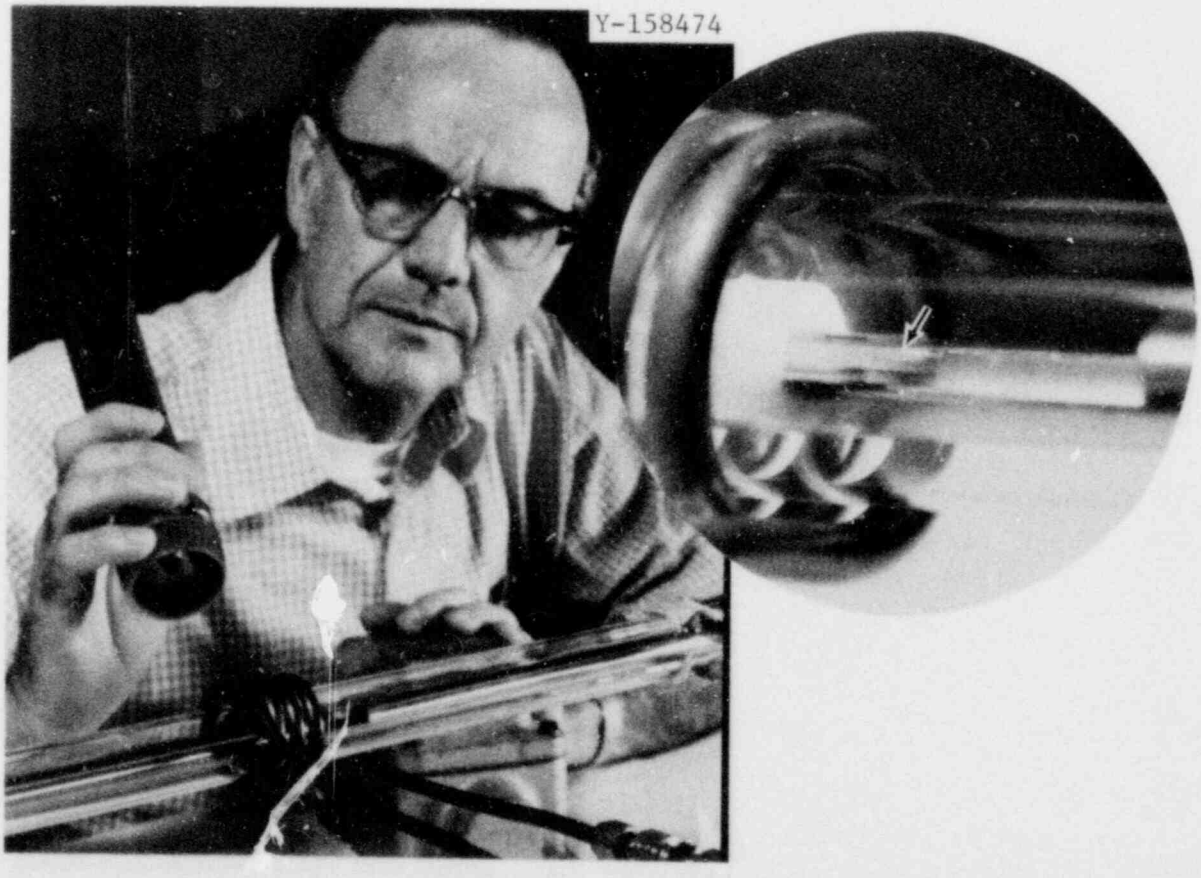

Fig. 26. Induction Brazing of a 1-mm-diam Thermocouple, which Protrudes Through the Wall of the Instrumented Rod. The ceramic sleeve insulators over the central conductor extensions can be seen in the inset (arrow).

atmosphere. After insertion of the eight triaxial cables and four thermocouples into a rod, the thermocouples were bent into a 90° angle at the tip and guided through a close-fitting hole through the tube wall. A small ring of wire was wrapped aound the couple near its end inside the tube so that on brazing the junction would not protrude over 0.5 mm (0.02 in.) into the subchannel spacing to avoid interference with the grid spacer during bundle assembly. The brazing filler metal powder, which was a commercial nickel-base alloy, BNi-2 (Ni-7.0Cr-4.5Si-3.0Fe-2.9B), was mixed with an acrylic binder. This particular alloy was chosen because it adequately wet all the stainless steel components in the helium atmosphere, had low errosion tendencies on the thin sheath of the thermocouple, and was not as susceptible to displacement by the magnetic induction field as were some of the other nickel-base alloys. In addition, steam oxidation tests [9 h between 700 and 800°C (1290 and 1470°F) and 5 h between 800 and 840°C (1470 and 1540°F)] showed this filler metal to corrode at about the same rate as type 304L stainless steel.

The four triaxial cables at a given level are drawn back from the thermocouple location (inset of Fig. 26) so that the end seals will not be damaged by the brazing operation. The window area of a rod is enclosed in a quartz tube with split rubber stopper end seals to maintain an inert environment and allow the operator to observe the flow of the filler metal. The thermocouple brazes are inspected visually and by helium pressurization and alcohol immersion after the sensor subassemblies have been laser welded into place. Although it would be more desirable to leak check these brazes before sensor installation, this was not done because of problems involved with sealing the upper rod end (with all the cables passing through) and the window openings themselves. In fact, these brazes were usually very successful, both from leak tightness and electrical-integrity standpoints, and the few joints that looked questionable on visual inspection at 10× magnification were rebrazed before rod assembly continued.

Brazing of Upper Rod Termination

The final closure of the instrumented guide tube rods at the upper end, through which the eight triaxial cables, four thermocouples, and the

3.18-mm-diam (0.125-in.) vent tube pass, was a very challenging problem, although the only material involved was type 304L stainless steel. We did not seriously pursue a course of simply adding filler metal to and brazing the very tightly packed bundle because: (1) the relatively large interstitial spaces between cables preclude joint filling by capillary flow, and (2) placing alloy powder at the joint is difficult even if one of the brazing filler metals capable of bridging a wide gap is found to be suitable.

Our approach was to bend a jog in each of the cables so that they would spread in an expanded pattern allowing a machined grid plate to be used (Fig. 27). Without this operation the components are spaced too tightly for placement of alloy, and the web thickness of the end plate is too thin for fabrication.

Several different designs were evaluated for the termination fitting including both one and two-piece models. We initially tried high-frequency induction heating. However, we were unable to develop a fitting

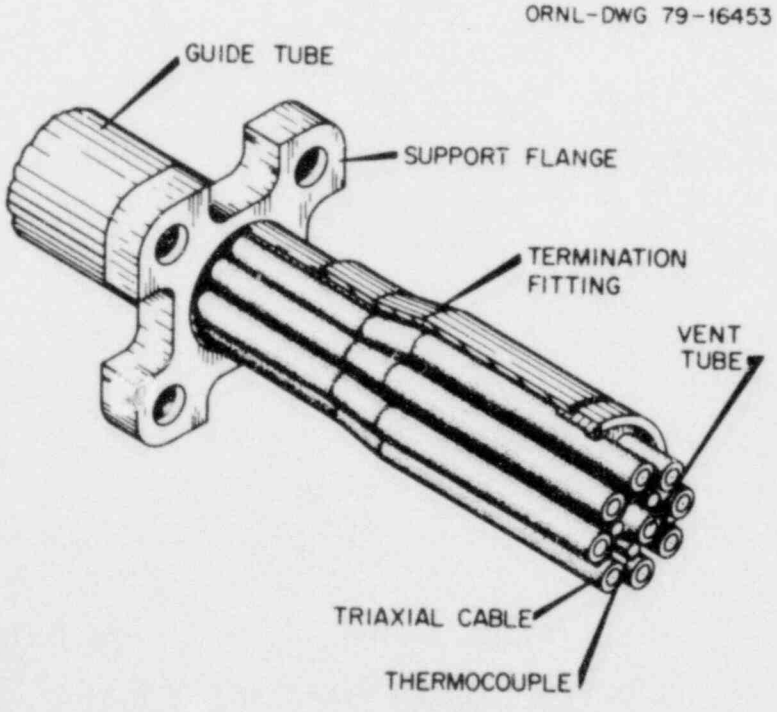

Fig. 27. Upper Rod Termination of AIRS Instrumented Guide Tube Assembly. All the joints are brazed simultaneously in a resistance-heated furnace with a commercial nickel-base filler metal (BNi-3). The support flange is tack-welded in place after brazing.

geometry and induction coil configuration that would result in even heating of the various components. Thus, although we occasionally produced a leaktight prototype assembly, we were unable to do this repetitively and so terminated our efforts in this area.

What we did find to be successful from the standpoint of both relative ease of assembly and excellent brazability was a furnace braze of the two-piece termination shown schematically in Fig. 27 and pictured in Fig. 28. The furnace shown in Fig. 16 was used for heating, but because of the difficulty in trying to make a vacuum-tight seal around all the cables that extend through one end of the tube we used a helium atmosphere. Helium is fed at a low rate [40 ml/s (5 cfh)] through the vent tube of the rod to purge out the internal oxygen, and the inside of the furnace tube is also blanketed with inert gas fed at 0.24 liter/s (30 cfh). Gas bleeds out through the bundle of cables and thermocouples as well as through the lower end of the rod. The brazing filler metal used is AWS-BNi-3 (Ni–3% B–4.5% Si), with the joint area held for 5 min at 1050°C (1920°F). The temperature is monitored by a thermocouple wired to the rod at the termination. Although this protective atmosphere is not of a very high quality (as evidenced by a light gray-to-green oxide layer after brazing) we have had very reproducible, leak-tight joints using this procedure. We think that

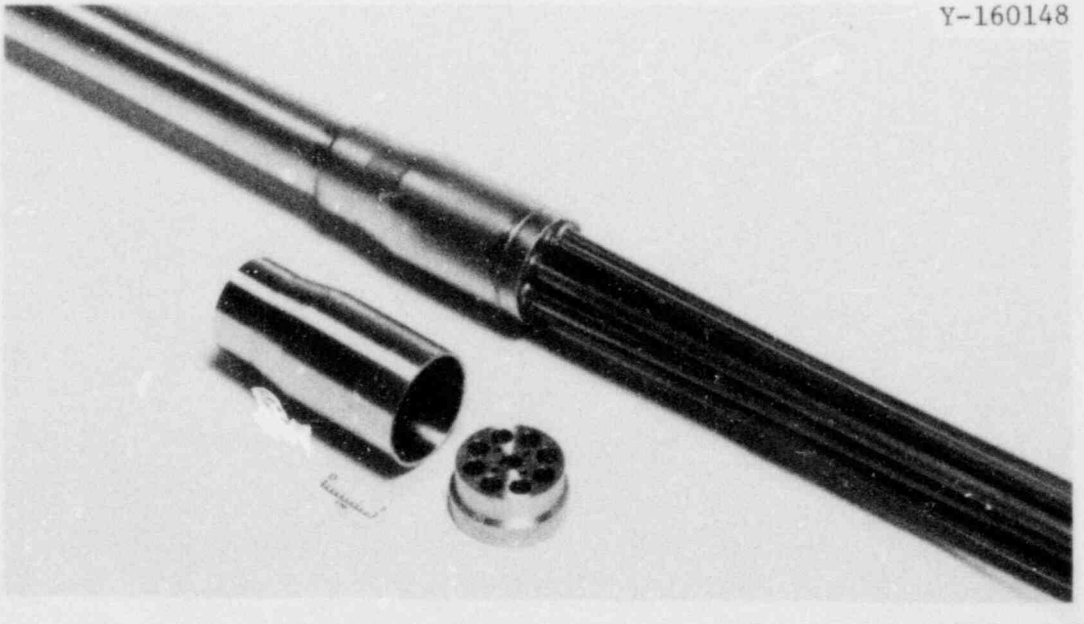

Fig. 28. Upper Rod Termination Components and Brazed Assembly. The rod support flange has not yet been welded into position.

because of the fast heating rate produced by the preheated furnace element that much of the oxide is formed after the braze is completed. Also, this filler metal is known to flow freely in marginal atmospheres. This alloy also tends to dissolve some of the stainless steel base metal, but because of careful time and temperature control we have not experienced problems with interaction of the molten metal with the thin sheaths of the thermocouples. Steam oxidation tests [9 h between 700 and 800°C (1290–1470°F) and 5 h between 800 and 840°C (1470–1540°F)] conducted on an inverted tee specimen of platinum and type 304L stainless steel brazed with BNi-3 showed that this filler metal was apparently as corrosion resistant as the stainless steel.

Final Assembly Operations

After the upper rod termination has been brazed, the sensor subassemblies, which were previously wired into place, are then laser welded into the rod. This operation is delayed until this time so that if a major problem encountered in brazing of the termination precludes use of the rod, then the sensor modules can be removed and used in another assembly. The tapered lower end plug and the rod support bracket are gas tungsten-arc welded into position, and the completed instrumented guide tube assembly (shown schematically in Fig. 29) is then ready for final electrical and leak check tests.

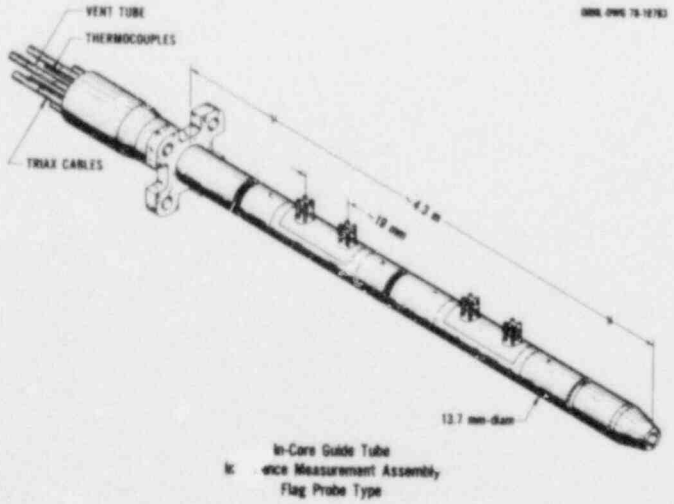

Fig. 29. Flag Probe Impedance Measurement Assembly as Shipped to Germany for Installation in the PKL Reflood Test Facility.

Fabrication and Testing of Instrumented Rods

Subsequent to the development of the cermet material and above-described joining techniques, we assembled nine of the 4.3-m-long (14-ft) (8.6 m including cables) instrumented guide tube rods for impedance measurements in two-phase flow test systems. Of this total two were of the prong probe design and the balance flag probe sensors. Five of the rods (some of which are shown in Fig. 30 and 31) were successfully operated at relatively low temperature [175°C (350°F)] in a steam-water test stand at Oak Ridge to evaluate the performance of the sensors and associated instrumentation. Four of the five assemblies maintained their structural integrity during these tests (which were admittedly much less severe than

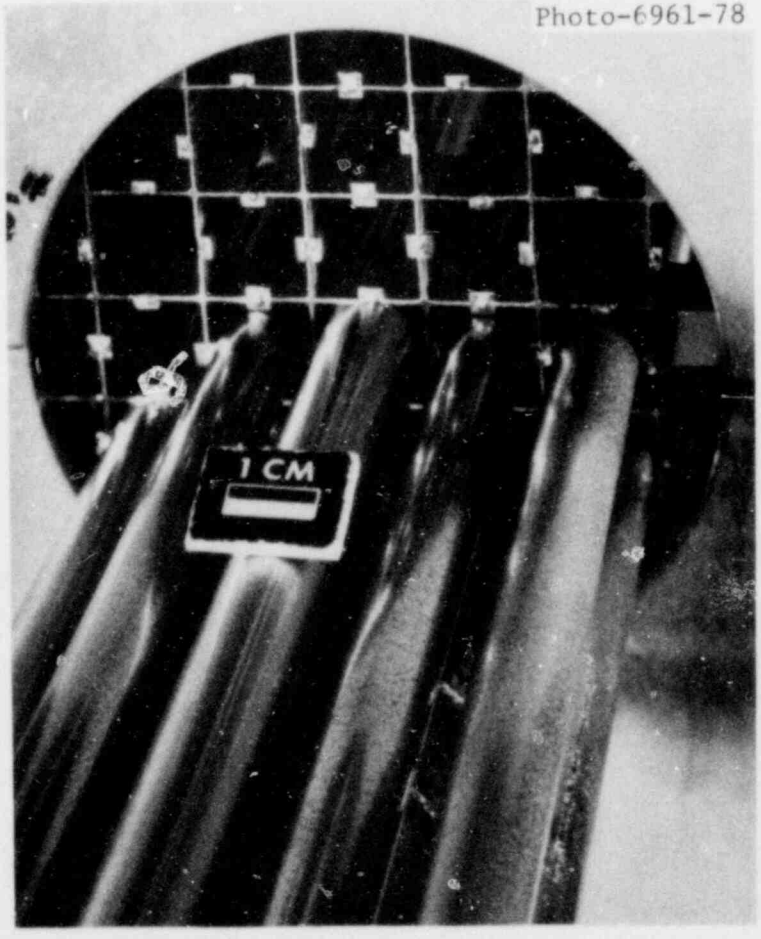

Fig. 30. Partially Assembled Bundle of Instrumented Guide Tube Rods and Dummy Fuel Rod Simulators.

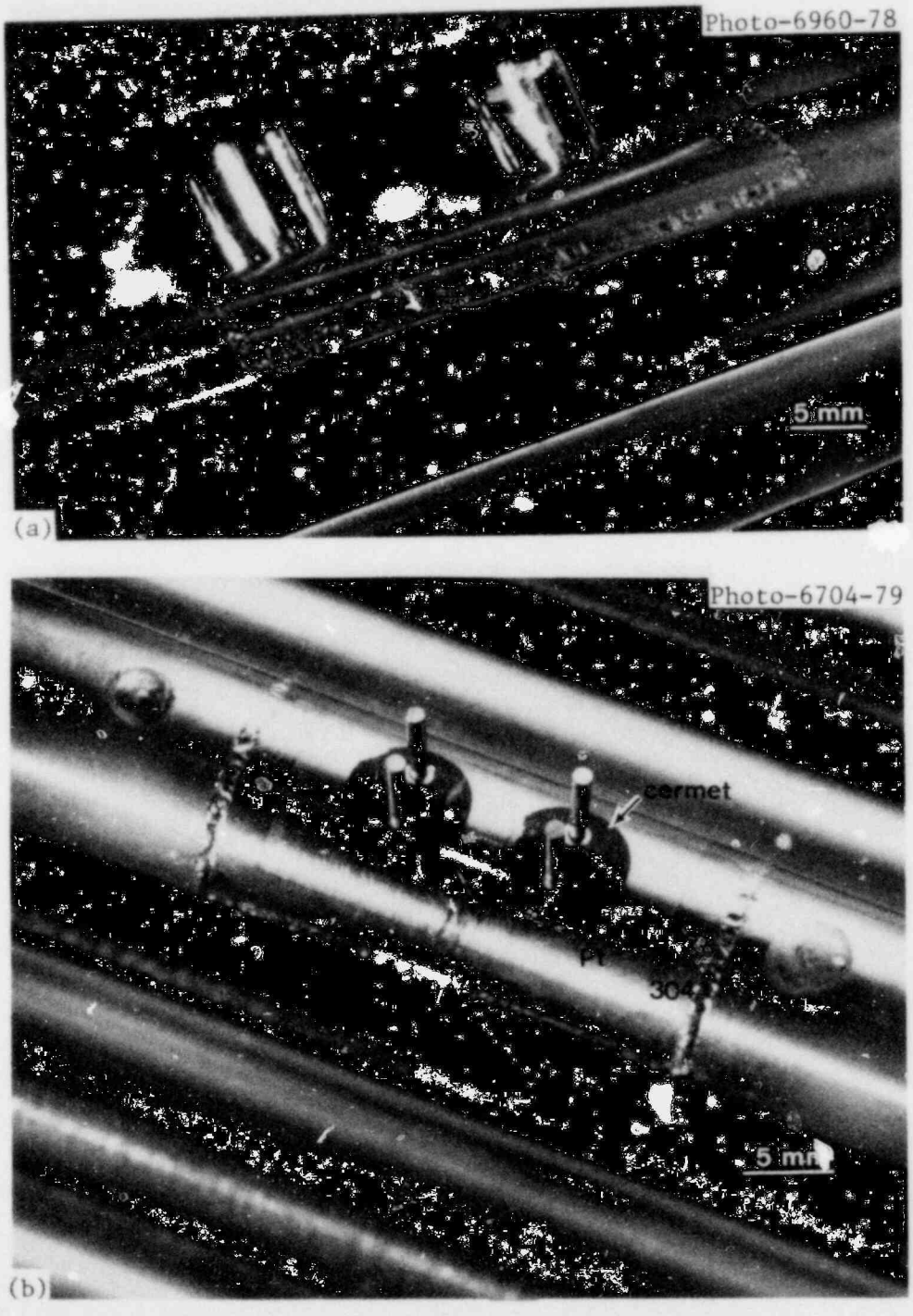

Fig. 31. Sensors on Instrumented Guide Tube Rods Shown Before 175°C (350°F) Steam-Water Tests at ORNL. (a) Flag-type probe on rod IF48-5. (b) Prong probe on level 7 of rod IP67-13.

the conditions in a reflood facility), but one rod did develop a sizeable leak. This occurrence was not without benefit, however, because we found that the performance of that rod was not affected by the leak because the brazed end seals kept the steam out of the cables.

These tests did reveal the need for further instrument development, and the rods themselves were damaged on removal from the test array. This damage required the replacement of the sensor subassemblies in some cases and the insertion of a stainless steel mesh packing material (to limit cable movements, which can cause platinum lead breakage) in all the rods above each sensor location. The latter modification was accomplished by machining a 6.35-mm-wide (0.250-in.) slot on the backside of the rods at two locations (just above the upper thermocouple at each level), forcing in a semicircular ring of stainless steel mesh, and then laser welding a door into each opening. After these changes, two of the tested rods and three new units were shipped to Germany, where they have been assembled in a test bundle for installation in the reflood facility.

MODIFICATIONS TO SENSOR SUBASSEMBLY DESIGN

Although we were able to successfully build and test the above described instrumented assemblies, it became apparent that the design of the flag probe sensor subassemblies needed improvement, as our reject rate on these components (due to leakage after final machining) was excessive. After careful analysis we concluded that our difficulties resulted from the mismatch in coefficients of thermal expansion of the components and from the free flowing of the brazing filler metal on the insulator. The thermal expansion mismatch had been partially accommodated by use of the platinum transition piece, but the subassembly still distorted significantly during brazing (0.38 mm at the center of the 38-mm-long part) and was returned to contour only by straightening in a press and then grinding the outer surface. The excess filler metal was thus ground from the outer surface, but on the inside a diamond-tipped core drill was used to remove a circular path of alloy from around each plug (see Fig. 24). We concluded that leaks through the braze joints and cermets were caused by both straightening and core drilling, so we undertook a task to eliminate these operations.

The first modification to the flag probe sensor subassembly was to increase the amount of stainless steel in the axial direction to decrease the length of the lower expansion transition material (platinum) so that the distortion on heating would be les . This was accomplished (Fig. 32) by using two platinum transition pieces rather than one, with a combined

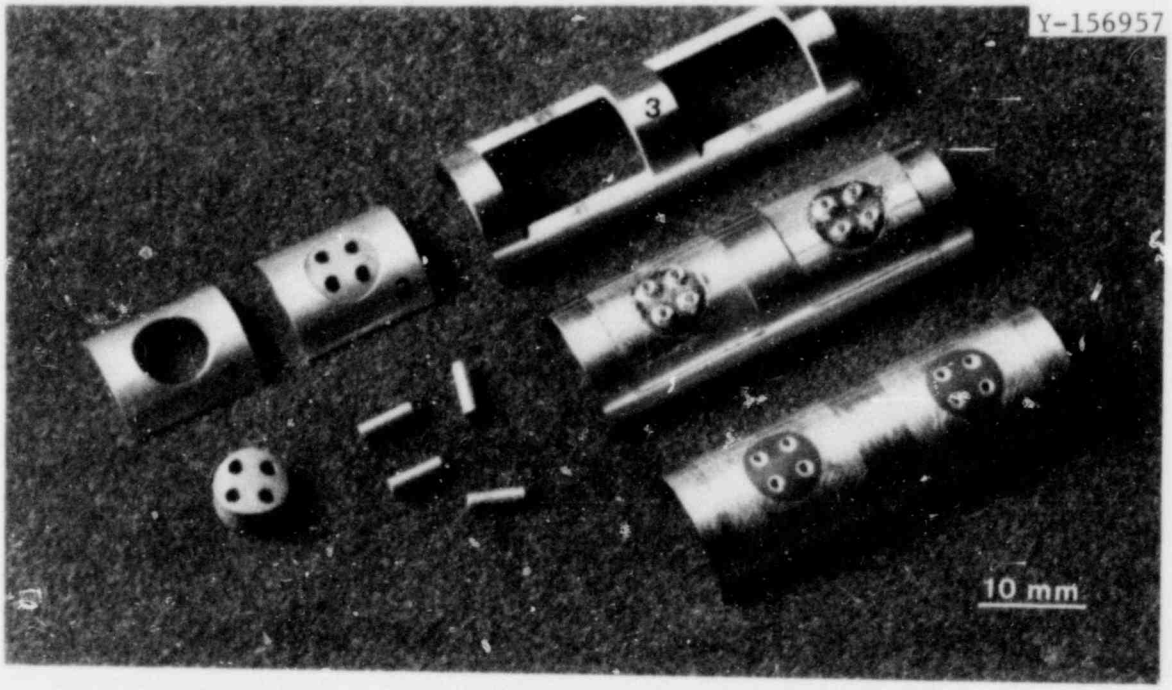

Fig. 32. Flag Probe Sensor Subassembly Modified to Reduce the Amount of Distortion in This Dissimilar Material Component by Using Two Smaller Platinum Transition Pieces (Labeled 1 and 2). Part of the platinum in the former design is replaced by stainless steel, 3.

length of 27.4 mm (1.08 in.) instead of 32.5 mm (1.28 in.). This change resulted in significantly less distortion [0.25 vs 0.38 mm (0.010 vs 0.015 in.)] and in fact two of the three untested rods that were shipped to Germany in the fall of 1978 contained one or both sensor subassemblies of this design. Although this amount of radial deflection in the dual transition piece subassembly still necessitated a straightening operation, the reduced magnitude required led to a significant improvement in the modules. Of ten flag probe subassemblies brazed with the single platinum transition, seven had one or more leaks [as determined by pressurizing internally with 0.14 MPa gage (20 psig) He and immersing in alcohol to

detect any bubbles]. About half the parts leaked at one or more of the platinum sensor support plugs. By comparison, when six subassemblies with the dual platinum transition were leak checked, three had leaks, and two of these had only very small leaks.

In order to reduce the amount of distortion in the sensor modules still further, we subsequently changed from a type 304L to a type 446 stainless steel frame. The latter is a ferritic stainless steel and, therefore, magnetic, but this will not be a problem in the impedance tests. This change was made because type 446 has a mean coefficient of thermal expansion [0 to 1000°C (32–1830°F) of 13.7×10^{-6}/°C (7.6×10^{-6}/°F compared with 20.2×10^{-6} (11.2×10^{-6}) for the austenitic type 304L.[10] With the type 446 frame and the dual platinum chip design, the maximum distortion at the center of the 38-mm-long subassembly was 0.08 mm (0.003 in.), and this slight amount eliminated the need altogether for the straightening operation.

We also took another step to reduce the potential for damage to the cermet when the core drill was used to remove brazing filler metal from around each platinum plug on the inside of the module. Instead of core drilling we removed the excess alloy by abrasive grit blasting, and optically we could see that this process did not cause the cracking and chipping in the cermet as had generally been seen after core drilling. The change to grit blasting appears, in retrospect, to have made the significant improvement in quality of the sensor subassemblies. However, only two modules were tested with a type 446 stainless steel frame and core drilling around the plugs (both of which leaked), so it is hard to isolate the impact made by the change to type 446 alone. Nevertheless, of five subassemblies fabricated with dual platinum transitions, a type 446 stainless steel frame, and grit blasting to remove excess alloy on the inside, all were helium bubble tight.

The final modification to the design of the flag probe sensor subassembly was to eliminate half the through-holes in each of the cermet insulators. As previously mentioned, the function of one plug out of each pair is merely to support the end of the flag, so we took advantage of this fact to reduce the number of possible leak paths. This modification, which is shown in Fig. 33, also reduces the congestion inside the rod by eliminating the four protruding plugs. Five subassemblies were made

having type 446 frames and the two through-hole cermets, and all were helium bubble tight after grit blasting and final machining.

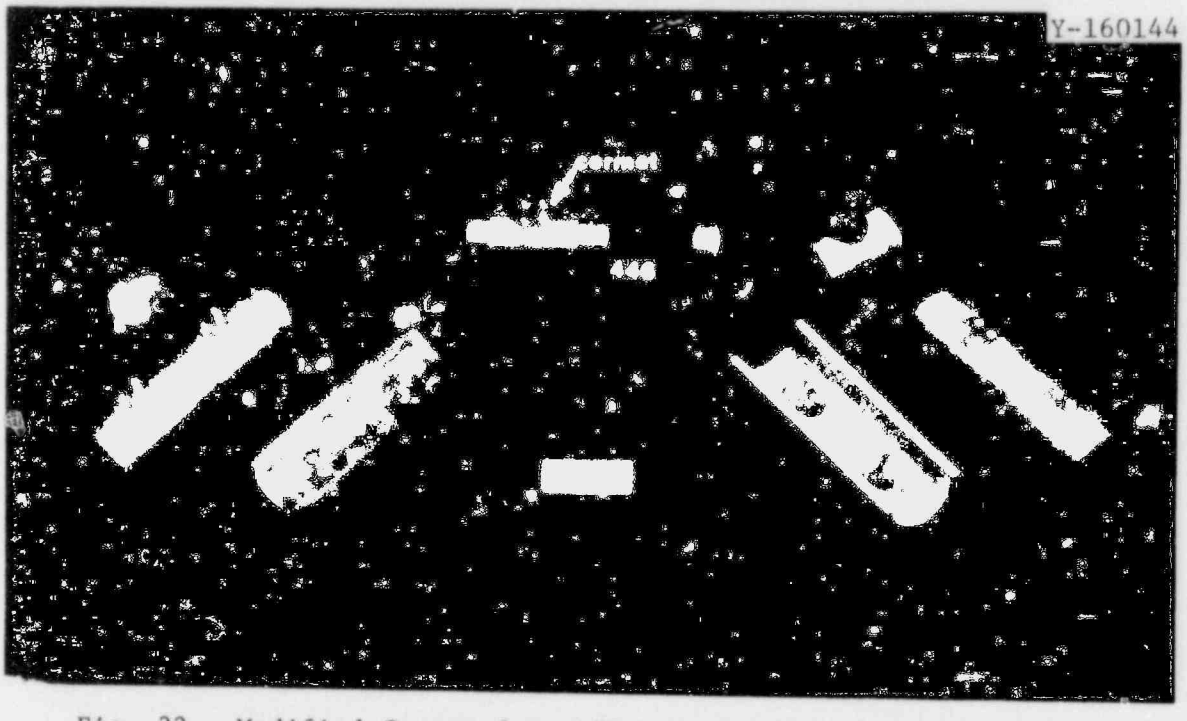

Fig. 33. Modified Cermet for a Flag Probe Sensor Subassembly, in which Only Two Platinum Electrode Support Plugs Pass Through the Cermet. The remaining two plugs in each insulator are brazed into blind holes. Note the smooth contour (arrow) where the excess filler metal has been removed by abrasive grit blasting.

ACKNOWLEDGMENTS

The authors would like to express their appreciation to the following individuals who made significant contributions to this work. N. D. McCollough, J. A. Williams, and L. D. Hunt of the Instrument and Controls Division assisted in rod assembly and performed the electrical and leak tests. W. R. Johnson of the Ceramic Technology Group of the Metals and Ceramics Division made all the experimental cermet materials. D. L. Fahey and T. L. Marlar of the Metallography Group were the photographers, and C. P. Haltom was the metallographer. The manuscript was reviewed by J. W. McEnerney and J. O. Hylton. The final report was edited by S. Peterson and prepared for reproduction by A. Rice.

REFERENCES

1. B. G. Eads et al, *Advanced Instrumentation for Reflood Studies Program Quart. Prog. Rep., Dec. 31, 1977*, ORNL/NUREG/TM-202.
2. C. S. Morgan, "*In-Situ* Deposition of Metal Coatings," *Thin Solid Films* 39: 305–11 (1977).
3. C. E. Holcombe, *Properties of Thermally Contracting Tantalum Tungstates*, Y-2071 (February 1977).
4. L. Reed, "Ceramic To Metal Sealing," pp. 34–43 in *Electronic Ceramics*, Special Publication 3, American Ceramic Society, Columbus, Ohio, May 1969.
5. W. H. Kohl, *Handbook of Materials and Techniques for Vacuum Devices*, Reinhold, New York, 1967, pp. 446–51.
6. R. G. Donnelly and G. M. Slaughter, "The Brazing of Graphite," *Weld. J. (N.Y.)* 41(5): 461–69 (1962).
7. C. W. Fox and G. M. Slaughter, "Brazing of Ceramics," *Weld. J. (N.Y.)* 43(7): 591–97 (1964).
8. D. A. Canonico, N. C. Cole, and G. M. Slaughter, "Direct Brazing of Ceramics, Graphite, and Refractory Metals," *Weld. J. (Miami)* 56(8): 31–38, (1977).
9. A. J. Moorhead, R. W. McCulloch, R. W. Reed, and J. J. Woodhouse, *Development of Joining Techniques for Fabrication of Fuel Rod Simulators*, ORNL report in preparation.
10. T. Lyman et al, eds., *Metals Handbook*, 8th ed. Vol. 1, American Society for Metals, Metals Park, Ohio, pp. 422–23.

NUREG/CR-1359
ORNL/NUREG-65
Distribution
Category R5

INTERNAL DISTRIBUTION

1–2. Central Research Library
3. Document Reference Section
4–5. Laboratory Records Department
6. Laboratory Records, ORNL RC
7. ORNL Patent Section
8. Nuclear Safety Information Center
9. S. I. Auerbach
10. R. L. Beatty
11. A. J. Caputo
12. W. R. Casto
13. R. H. Chapman
14. B. G. Eads
15. D. P. Edmonds
16. T. G. Godfrey
17. G. M. Goodwin
18. D. E. Harasyn
19. M. B. Herskovitz
20. R. F. Hibbs
21–22. M. R. Hill
23. H. Inouye
24. W. J. Lackey
25. R. W. McClung
26. R. E. McDonald
27–31. A. J. Moorhead
32. C. S. Morgan
33. M. L. Myers
34. F. R. Mynatt
35. G. W. Parker
36. A. E. Pasto
37. R. W. Reed
38. G. M. Slaughter
39. V. J. Tennery
40. G. C. Wei
41. J. J. Woodhouse
42. A. L. Bement, Jr. (Consultant)
43. W. R. Hibbard, Jr. (Consultant)
44. E. H. Kottcamp, Jr. (Consultant)
45. M. J. Mayfield (Consultant)
46. J. T. Stringer (Consultant)

EXTERNAL DISTRIBUTION

47. NRC, Office of Nuclear Regulatory Research, Washington, DC 20555
Program Sponsor

48. DOE, Oak Ridge Operations Office, P.O. Box E, Oak Ridge, TN 37830
Office of Assistant Manager, Energy Research and Development

49–50. DOE, Technical Information Center, P.O. Box 62, Oak Ridge, TN 37830

51–410. For Distribution Category R5.

☆U.S. GOVERNMENT PRINTING OFFICE: 1980-640-245/029